Welcome Lecture

Brazilian research and practice with geosynthetics

Sandroni, S.S.
Geoprojetos Engenharia Ltda, Rio de Janeiro, RJ - Brazil

de Mello, L.G.
Vecttor Projetos, São Paulo, SP; Assist. Professor, University of São Paulo, SP - Brazil

Gomes, R.C.
Associate Professor, Federal University of Ouro Preto, MG - Brazil

Vilar, O.M.
University of São Paulo, São Carlos, SP – Brazil

Keywords: geosynthetics, Brazil, reinforced soils, drainage, dewatering, landfill, liner

ABSTRACT: Geosynthetics are worldwide used in many engineering applications. Their versatility and constructive easiness has improved the design and construction of many geotechnical projects. This text presents a broad view of the Brazilian experience in the use of geosynthetics in reinforced soil structures, mining applications and landfilling. Practical cases, together with the results of research activities recently developed are addressed

1 INTRODUCTION

The advent of geosynthetics has improved design and construction issues in Engineering. Geosynthetics are known for their versatility, low cost and constructive easiness and have become a basic component in the design and performance of many applications in the mining industry, residues and effluent disposition, soil reinforcement and drainage, among others. Their use is spread worldwide and they are, nowadays, in routine use in most geotechnical job sites in Brazil, as in other countries. Brazilian Standards, which encompass testing and guidance for design with geosynthetics, are either in use or under discussion. There is an active chapter of International Geosynthetics Society (IGS); and ABINT, the Brazilian geosynthetic producer's organization, is no less active. It has sponsored the Brazilian Manual of Geosynthetics (ABINT, 2004), a reference book on materials and design procedures, largely used in practice. Up to now, five Brazilian Geosynthetic Conferences have been held.

This paper deals with the Brazilian experience in the design and construction with geosynthetics, focusing mainly on their use in soil reinforced structures, in the transportation and mining industry and in the final disposition of residues, including those from mining activities and urban areas.

Topics on soil reinforced structures address stability of geotextile reinforced fills, fills on geogrid platform on piled concrete caps and fills on geotextile encased columns (GEC).

Regarding the use of geosynthetics in the mining and transportation industry, the following aspects are focused: reinforced walls for tailing ponds, reinforced slopes in highways, geosynthetics in pavements, railways with heavy loads, drain, filtration and dewatering of tailings.

Finally, the use of geosynthetics in the disposition of residues is addressed, showing examples of common liner alternatives, together with their use in the rehabilitation of old dumps and residues deposits.

The text was devised to present a broad view of Brazilian experience on the use of geosynthetics, focusing in practical cases and recent research activities and was divided in three parts: Reinforced fills in very soft clay sites; Geosynthetics and mining residues in geotechnical applications and Geosynthetics in landfill.

2 REINFORCED FILLS IN VERY SOFT CLAY SITES

2.1 *Introduction*

Major Brazilian universities (e.g. UNB in Brasilia, COPPE and PUCRJ in Rio de Janeiro, USP in São Carlos, etc) have research lines on geosynthetics and well equipped laboratories. Part of the recent research efforts in Brazil have been directed towards measurement of strains and forces in geosynthetic layers used to hold or reinforce fills in sites with very soft organic clays, which is the chosen subject. The following aspects will be addressed in what follows:

- stability of geotextile reinforced fills;
- fills on geogrid platform on piled concrete caps;
- fills on geotextile encased columns (GEC).

2.2 *Stability of geotextile reinforced fills*

2.2.1 Practice and Research on geotextile reinforced fills

Brazilian design practice for stability of reinforced fills on soft clays follows internationally accepted design procedures such as those described by Rowe and Li (2002). As a rule, the contribution of the geosynthetic reinforcement is computed as an additional resisting force in limit equilibrium analyses. Less frequently, numerical stress-strain analyses (usually, FEM) are carried out, in addition to limit equilibrium.

Magnani de Oliveira (2006) presents the results of three instrumented clean sand embankments, built over a soft clay deposit, taken to failure at Florianópolis, Santa Catarina, named T1, T2 and T3. Fills T1 and T2 have been reinforced with one layer of woven polyester geotextile (brand name stabilenka) with T_{ult} = 200 kN/m and $J_{5\%}$ = 1700 kN/m. Fill T1 had prefabricated vertical drains in the soft layer (triangular array, with 1,30 m spacing), fill T2 did not have PDVs and fill T3 had neither reinforcement nor PVDs.

The behavior of fill T2 (with reinforcement, no PDVs) will be focused. It has been taken to failure in about 45 days. Cross section in figure 2.1 shows the subsoil layers, the topographical surface of the embankment (initial and after failure), the location of the instruments and the position of the failure surface. The original ground profile consisted of a 6 m thick soft clay layer (with water content around 130%, Cc/(1+e) of the order of 0,40 and undrained strength around 10 kPa), underlying a 1 to 2 m thick hydraulically placed clean sand layer and overlying a clean sedimentary sand layer. The geotextile reinforcement was placed after about 1 m of the fill had been built (the "initial sand layer" shown in figure 2.1). Vertical displacements, horizontal displacements and tension on the reinforcement have been measured in several positions. Details can be found in a paper to this conference (Magnani de Oliveira et al, 2010).

Figure 2.2 shows the progress of fill heightening and settlements with time. Displacements accelerated after placement of 8th layer. Complete failure, with appearance of tension cracks at fill surface and distinct increase in displacement velocities, happened just after placement of the 10th layer. "Failure" can be considered to have happened upon application of the 9th layer, with fill a little thicker than 3 meters.

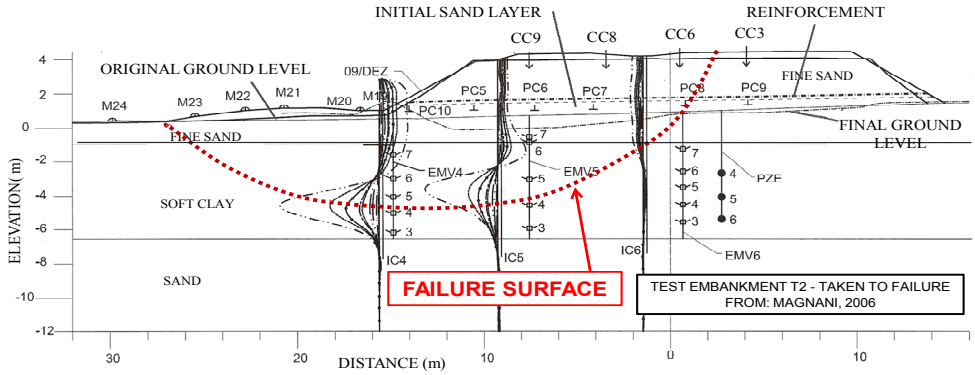

INSTRUMENTS: CC – REINFORCEMENT LOAD CELLS; M – SURFACE SETTLEMENT MONUMENTS; PC – SETTLEMENT PLATES; PZE – ELECTRIC PIEZOMETER; EMV – MAGNETIC DEEP SETTLEMENT INDICATOR; IC - INCLINOMETER

Figure 2.1. Section of fill T2 (Magnani de Oliveira, 2006)

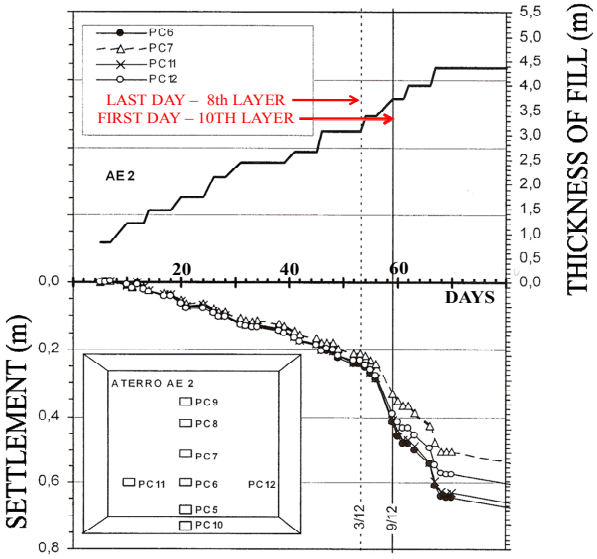

Figura 2.2. Load sequence and settlements – Fill T2 (Magnani de Oliveira, 2006)

Figure 2.3 shows the development of horizontal and vertical displacements as loading progressed, emphasizing the 9th layer.

Figure 2.4 presents the reinforcement tensions (in kN/m) measured with planar load cells, specifically developed at Prof. Mauricio Ehrlich's laboratory in Coppe/UFRJ for Magnani de Oliveira's research, shown in figures 2.5 and 2.6. The load cell measurements indicated that, when the failure process began (8th layer), the tension in the geotextile at the point of interception with the failure surface, was around 10 kN/m (corresponding to about 5% of its tensile strength). Tension at the intersection increased to about 30 kN/m (15% of the tensile strength), after failure, when the fill height had increased to the 10th layer and large failure displacements where taking place. Therefore, during failure, the "safety factor" of the fill is around 1 whilst the "safety factor" of the reinforcement is somewhere above 10 or, somewhere above 4 or 5, after applying reduction factors associated with manufacturing defects, damage during construction, creep and environmental degradation, as indicated, for example, in BS8006 (1995).

Currently available limit equilibrium codes, for example Geo-Slope (2007), allow choosing a given value, direction and point of application for the mobilized tensile force in the reinforcement. There seems to be agreement among specialists that the reinforcement should be considered as acting along its original direction, usually horizontal, at the location where the failure surface crosses the reinforcement (Rowe & Li, 2002). There also seems to be general agreement that, rather than using different values of safety factor for soil and reinforcement, it is preferable to establish a value for the force (traction) that will develop in the reinforcement.

There are simplified methods to estimate the force in the reinforcement such as, for example, Rowe & Soderman (1985) and Low and others (1990). Alternatively, one could carry out a FEM analysis to estimate the traction force. In general, the more sophisticated codes (such as Cam Clay and Cap models) are required.

Rowe & Soderman's (1985) procedure requires the geometry of the fill, unit weights of the materials, and average values of the undrained strength (Su) and of the relation between undrained modulus and undrained strength (Eu/Su) of the soft soil. For a given set of parameters one obtains an estimate of the strain in the geosynthetic which, multiplied by the elected geosynthetic modulus (J), yields the estimated traction load. Adopting γ_f.Hc = 60 kPa, Su = 10 kPa and Eu/Su = 300, Magnani de Oliveira et al (2010) obtained a strain of 1.6% which, multiplied by J = 1700 kN/m, results in a force equal to 27.2 kN/m for the reinforcement of fill T2 upon construction of the 9th layer. This value should be compared with values between 19 kN/m (at the intersection of the fill with the reinforcement) and 33 kN/m (maximum measured traction), for the 9th layer shown in figure 2.4. This agreement must be considered as surprisingly good.

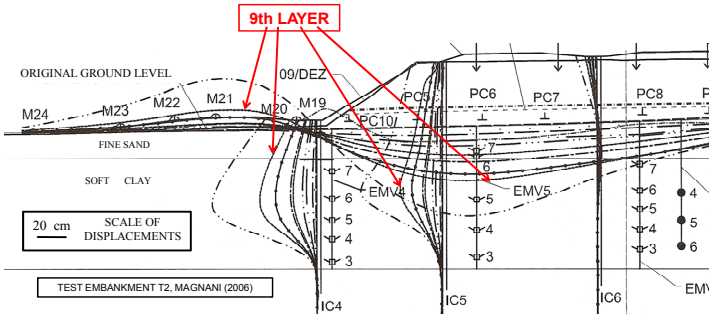

Figure 2.3. Displacements of fill T2 (Magnani de Oliveira, 2006)

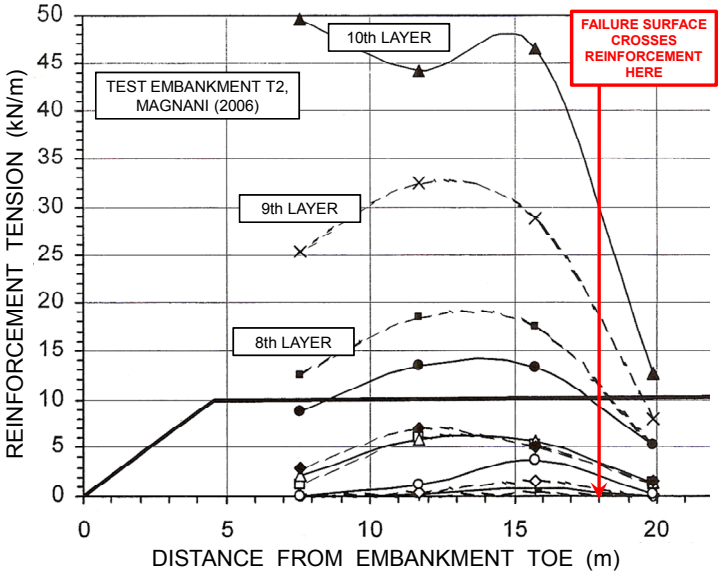

Figure 2.4. Tension at reinforcement – Fill T2 (Magnani de Oliveira, 2006)

Low and other's (1990) procedure requires the geometry of the fill and the value of safety factor without reinforcement for different depths of the failure surface. The method yields a value of the traction force, T, in the geosynthetic. Using the same parameters as above and adequate non-reinforced safety factors one finds T around 150 kN/m. As can be seen there is a very large contrasts among the calculation methods.

The choice of the resistance of the reinforcement also depends on what is considered acceptable behavior of the fill. There are situations in which it is acceptable to have cracks, without vertical steps, in the fill and to wait for strength gain in the soft clay before the desired pavements, structures, utilities, etc are built. This is the case of many road fills and of some industrial and residential fills with flexible time schedule. Under such conditions it is not necessary to use reinforcement with strength much above the expected tension and the tension can be estimated in a less imposing manner.

On the other hand, in situations where only very small displacements can be tolerated and available time is scarce, some practitioners believe that in-

creasing the rigidity and, as a consequence, the strength of the reinforcement is effective in reducing strains and gaining stability. Of course, as far as stability is concerned, there is a limit for benefit, once the "perfectly reinforced" situation is reached and failure by sliding is replaced by bearing capacity (or "squeezing") failure. In situations in which heavy reinforcement is considered, consideration is usually also given to other design postures such as treatment of the soft soil with dry or wet mixing, granular columns and piled concrete slabs.

Time is also a design issue: on one hand there is the gain in strength due to consolidation and, on the other hand, the decrease in traction due to creep in the geosynthetic. It is possible that the minimum safety factor does not coincide neither with the "undrained" (end of fill construction) nor with the long term situations (see, for example, Abramento, Castro & Campos, 2002; Vidal, Silva & Queiroz, 2002).

The selection of the strength of the reinforcement for fills on soft soils is surely a question demanding further research and well documented case histories.

The presence of the geosynthetic reinforcement is beneficial to stability, increasing the thickness that a given fill can be built at a certain site with a given slope and construction velocity, as indicated by experience in a great number of jobs, in Brazil and elsewhere.

The presence of the reinforcement has the additional favorable function of minimizing the occurrence of the large vertical steps that are observed in failed unreinforced embankments on soft soils. Fill T2 did not present steps after failure (see figure 2.7). The same absence of steps was observed at fill T1 (reinforced). Fill T3 (no reinforcement) presented vertical steps some 50 cm high as shown in figure 2.8.

2.2.2 Failure of a geogrid reinforced fill

A slip failure on a geogrid reinforced fill on very soft organic soil occurred in a job in Rio de Janeiro. The designer calculated stability and reinforcement bond length using the procedures suggested by Low et al (1990). Failure happened along a surface located just behind the reinforcement layer. The failure steps shown in Figure 2.9 coincide with the end of the reinforcement layer. Figure 2.10 presents a typical section and a photo with the detail of the failure surface next to the reinforcement. A back-analyses, shown in figure 2.10, with a failure surface passing just beyond the reinforcement and using the designer's geotechnical model as for geometry, layers and soil parameters, yielded a safety factor inferior to unity. This indicates that the external stability has not been verified and, suggests that the designer believed that the reinforcement bond length obtained with Low's method would also satisfy stability for failure surfaces passing beyond the end of the reinforcement. Of course, the bond length obtained following Low et al, 1990 or any other design method, may not be enough to guarantee global stability and, therefore, stability calculations for failure surfaces passing beyond the reinforcement must always be carried out.

2.3 *Fill on geogrid platform on piled concrete caps*

2.3.1 Practice and Research

Aubeny, Li and Briaud (2002) pointed out several design aspects of geosynthetic reinforced pile supported embankments which need improvement such as lateral movement, shear and bending moments in the piles, slope stability including the beneficial effect of piles, settlement of the fill and design of the geogrid platform (or "mattress"). This last aspect will be focused in the discussion that follows.

Current design methods for geosynthetic platforms resting on piled caps (e.g. BS8006, 1995; Kempfert et al, 2004) consider arching of stresses in the fill, uniform vertical stress in the gap between caps and uniform strain in the geogrid. As shown with 3D FEM studies by Villard, Kotake and Otani (2002) strain and stresses in the geogrid are by no means uniform.

Spotti (2006) presents strains measured at several points of a single layer geogrid (polypropylene coated PVA with 200 kN/m x 200 kN/m) resting on piled concrete caps (piles in square array 2,5 m x 2,5 m; square 0,8 m caps) and supporting a 1,50 m thick soil fill. The precast concrete piles were driven to refusal. In the instrumented test sections, the space below the geogrid was left void to allow immediate deformation of the reinforcement.

Figures 2.11 and 2.12 show the strain cell utilized by Spotti (2006), which has been developed specially for his research, at Prof. Mauricio Ehrlich's laboratory in Coppe/UFRJ. Figure 2.13 shows the geometry of the test and the measured strains. It is seen that strains are different in different locations of the geogrid and, that the strain varies with direction in the same location. Strains at the border of the pile caps are of particular interest, as they are distinctly higher than elsewhere.

2.3.2 Case history of geogrid platform on piled concrete caps

In a job site adjacent to the site presented above, a 1,5 m-high fill with a geogrid (200 kN/m x 200 kN/m) basal reinforcement resting on concrete caps (1,0 m x 1,0 m) bearing on precast concrete piles (in square array, 2,8 m x 2,8 m) driven to refusal has been constructed (Almeida et al, 2007; Almeida et al, 2008). A representative cross section is shown in figure 2.14.

The geogrid behaved well at some positions (figure 2.15) but has been tore at others (figure 2.16). Tearing of geogrids in this case appeared to start at

cap corners and to progress along cap edges until the geogrid was ripped in the full perimeter of the caps. It can be speculated that the causes for inadequate behavior were:

- Overstressing of the geogrid associated with settlement of the ground in between caps (see detail of figure 2.14). The ground between caps continues to settle under the weight of the fill, the contact between the geogrid and the ground surface is lost near to the caps and, as a consequence, there is no friction in the geogrid. Thus, intense, non-uniform strains and tensions develop in this part of the geogrid. Arching, also shown schematically in the detail of figure 2.14, induces increased normal stresses in the cap and in the region of the ground surface still in contact with the geogrid, creating "strong adhesion" of the geogrid by friction. The consequence of this process may be traction failure of the geogrid, particularly at the corners of the caps where the conceived mechanism would be the harshest.

- "Rubbing" of the geogrid at the edge of the cap associated to the cyclic loading of traffic, which may have been aggravated by the low relation between the height of the fill (1,50 m) and the span between pile cap edges (1,80 m).

Figure 2.5. Tension cells (Magnani de Oliveira, 2006)

Figure 2.6. Tension cells (Magnani de Oliveira, 2006)

Figure 2.7. Failure of reinforced fill (Magnani de Oliveira, 2006)

Figure 2.8. Failure of unreinforced fill (Magnani de Oliveira, 2006

Figure 2.9. Failure of fill with insufficiently long reinforcement

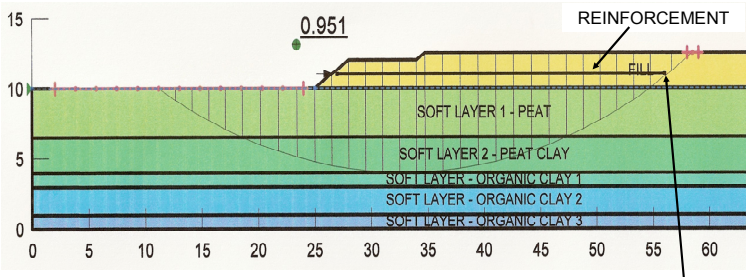

MATERIAL	γ (kN/m3)	C (kPa)	ϕ (degrees)
Fill	18	5	25
Peat	11	4	0
Peat clay	12	5	0
Org. clay 1	14	10	0
Org. Clay 2	14	14	0
Org. Clay 3	14	18	0

MORGENSTER-PRICE - CIRCULAR SURFACES

GROUND WATER = GROUND SURFACE

Figure 2.10. Typical section of failed fill with insufficiently long reinforcement

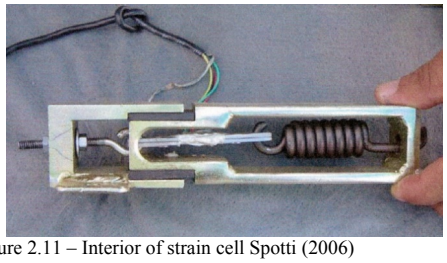

Figure 2.11 – Interior of strain cell Spotti (2006)

Figure 2.12–Instruments on site (Spotti,2006)

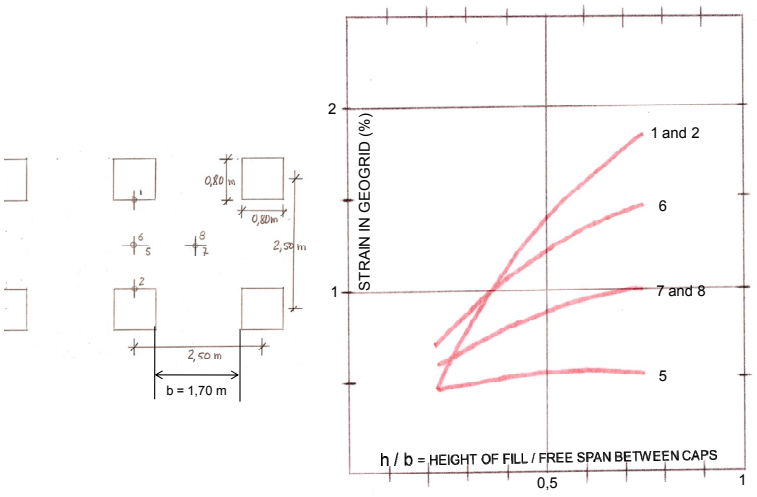

Figure 2.13. Layout of tests and strains measured by Spotti (2006)

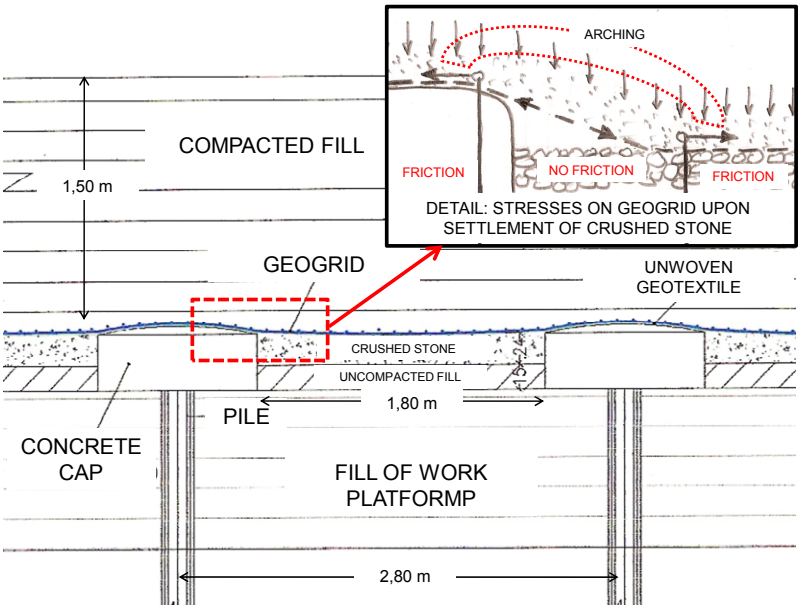

Figure 2.14. Typical section of geogrid platform on rigid piled caps

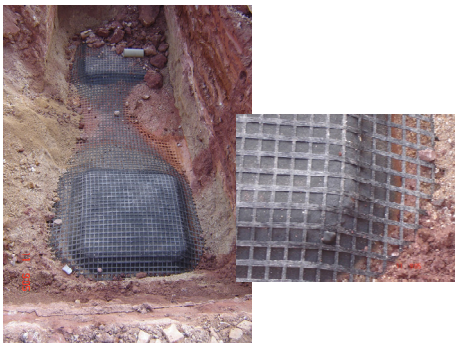

Figure 2.15. Good behavior of geogrid platform

Figure 2.16. Bad behavior of geogrid platform – geogrid teared at cap periphery

The above case indicates that direct contact between geogrids and rigid rough surfaces must be approached with caution.

Fills on geotextile platforms resting on piled concrete caps have also been used at the Panamerican Village. An instrumented test fill has been described by Sandroni & Deotti (2008). In the actual job, two layers of reinforcement have been used: a geogrid in contact with the concrete caps (fortrac; 200 kN/m in one direction) covered by a woven geotextile (stabilenka; 200 kN/m in the other direction). Due to excessive settlements, the fill had to be excavated in several points. No tearing was noted in a number of cases in which the geotextiles were exposed. The settlements have been caused by failure of the piles which did not offer enough bearing capacity for the loads that have been applied (which, in turn, were far greater than the design loads). Therefore, this case cannot be strickly taken as an example in which the geogrid did not tear at the cap corners, since the caps did not behave as rigid bearing points.

2.4 *Fill on geotextile encased columns (GEC)*

2.4.1 Construction of GECs and soil-column interaction

Geotextile encased columns (GEC) are columns of sand or crushed stone enveloped by a seamless geotextile with high rigidity (J between 1000 kN/m and 4000 kN/m). Regular use of GECs has started in Germany in the 90s following conceptions by Van Impe (1985, 1989). In Brazil GECs have been used in the last few years and are denominated “ringtrac columns” after the seamless geotextile producer’s brand name.

The construction sequence of the GECs is as follows: (a) insertion of a closed-end steel tube in the soft ground to the required depth; (b) placement of the geotextile inside of the steel tube; (c) filling up the tube with granular material; (d) opening the bottom of the tube; (e) vibratory withdrawal of the tube. In soils with undrained strength less than about 10 or 12 kPa it is possible to insert the steel tube in the ground by vibration, displacing the soft soil. In subsoil with higher strengths it is usually necessary to pre-excavate a hole, reducing the installation displacements but, on the other hand, creating the necessity of finding environmentally acceptable transportation procedures and final destination of the excavated soft soil.

Usual (nominal) diameters of GECs are 70 cm and 80 cm, but diameters of 60 cm and 1,00 m have been used. Its length can be virtually any up to 20 meters or more, depending on the capacity of the steel tube driving equipment. Heavy equipment may require a special work platform on very soft superficial soils. In Brazil, GECs with depths down to 12 m have been installed.

2.4.2 Practice with GECs

The behavior of a soft soil treated with GECs and loaded by a fill is a complex succession of interactions between the fill, the columns and the soft soil. The column is stiffer than the soft soil and, therefore, tends to attract load by arching. Under the increased load, the column tends to settle and to expand laterally. This lateral expansion, in turn, induces an increase in tension in the geotextile and an increase in lateral stress in the soft soil. Additionally, the columns perform as vertical drains, accelerating the consolidation in the soft soil mass. These events happen as a continuous process by the end of which the settlements virtually cease and the load sharing between the soft soil and the GECs tend to stabilize. Due to this complex interaction between the GECs and the soft soil two issues arise: (a) GECs in soft soil are considered, by most specialists, as a soil improvement method, as opposed to a system of load transfer to stiffer deep layers, such as concrete piles; (b) design calculations of GEC systems are quite complex and, as a consequence, most

practitioners require monitoring with adequate instrumentation to measure displacements.

The effect of GEC columns in reducing settlements can be empirically evaluated, in a very preliminary stage, using the graph given by Raithel, Hüster e Lindmark (2004), shown in figure 2.17, which relates the "improvement factor" (β =settlement without columns / settlement with columns), with the "area ratio" (α = area with columns / total area) and takes into consideration the stiffness of the geotextile (J). For the usual area ratios used in practice (say 10% to 25%), treatment with GECs seems to bring a two to five fold reduction in settlement.

Limited experience in Brazilian soft clays treated with GECs indicates that stabilization of settlements occurs a couple of months after placement of the fill.

As rule, a geogrid layer is placed at the level of the top of the columns, aiming to increase the lateral rigidity of the system, as well as, to help the distribution of stresses in the base of the fill.

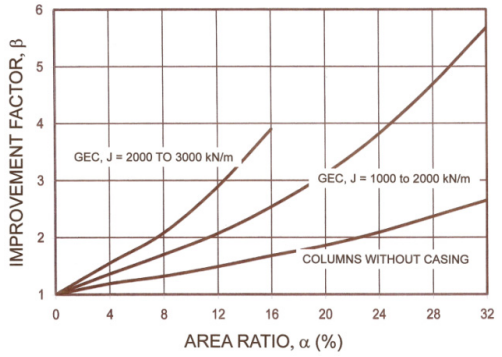

Figure 2.17. Raithel's graph for GECs

The theoretical treatment of GECs is complex due to the above mentioned interactions between the column, the geotextile casing, the soft soil and the embankment/geogrid. One must add to these complexities, the strong influence of the field procedures such as: the "looseness" of the geotextile inside the steel tube and the fact that the insertion of the steel tube remolds, to an unknown extent, the soft soil.

A practical aspect of concern is the condition of the granular material in the columns after construction of the GECs. Cone and SPT tests carried out inside GECs in a job site near Rio de Janeiro, before construction of the fill, indicate (see figure 2.18) roughly constant values of cone resistance and SPT from the depth of 3 m down to the bottom of a 10-meter deep column. This may be interpreted (see, for example, Schnaid, 2008) as indicating that either the relative density of the sand remained roughly constant (maybe due to "pluviation" effect of the sand during filling) or the presence of the geotextile induced an approximately constant horizontal stress with depth, with little external lateral reaction from the very soft soil, or both.

Design procedures for GECs can be numerical (FEM) or analytical (Raithel, 1999; Raithel and others, 2005; Kempfert e Gebresselassie, 2006). Raithel's method is based on the formulation proposed by Ghionna and Jamiolkovski (1981) including the geotextile. The formulation assumes the following simplifying hypotheses:

- Vertical displacements of the column and of the soft soil are equal;
- No displacements below the level of the base of the columns;
- The geotextile has linear elastic behavior;
- Soft soil has elastic behavior, with increasing stiffness with depth.

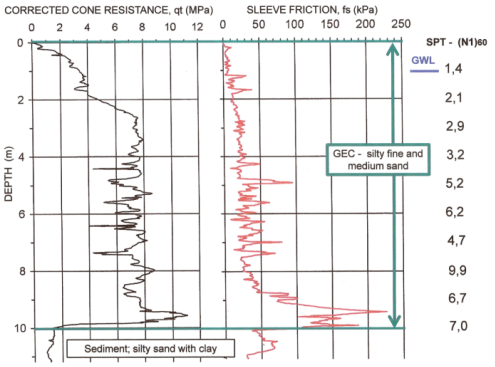

Figure 2.18. SPT and CPT tests inside GECs

Raithel's method requires the simultaneous resolution of two equations with 15 variables and 2 unknowns, Δr_c, the variation of the column radius and, $\Delta\sigma_{vs}$, the change in vertical stress in the soil. Once Δr_c is known, the expected settlement, which is considered equal in the soil and in the columns, can be estimated.

Since there is an arching effect implicit in Raithel's method, it should be used with caution if the thickness of the fill is less than the spacing between GECs and specific verifications should be carried out.

Currently in preparation, the EBGEO (German Recommendations for Geosynthetics Reinforced Earth Structures) will have chapter 6.10 devoted to GECs. A revision of BS 8006 is in the final stages at the time of writing.

2.4.3 *Case 1: GECs under road fill on soft clay*

The first application of GEC columns in Brazil, described by de Mello et al (2008a), was a 5 to 8.5 m-high fill for a road length of 140 m in São José dos Campos. The casing was a ringtrac 2000PM, woven geotextile with PVA and PA filaments in the peri-

meter and vertical directions, respectively. GEC were distributed in triangular array with spacing between 1,80 and 2,20m. Closed end steel tube was driven, causing displacement of the soft soil. The ringtrac geotextile had nominal diameter of 70 cm and rigidity, J, equal to 1000 kN/m. A basal geogrid layer (250x100 to 500x100 kN/m) was designed in the longitudinal direction considering the strength necessary for the embankment to develop arching between columns and, on the other hand, local stability.

Design of the lateral slopes reinforcement followed BS 8006 (1995). Horizontal equilibrium / stability was verified for different embankment heights, between 5 and 8,5 m, considering two different scenarios:

- full weight of the embankment loading the soft soil, considering the contribution of the sand columns improving average shear strength;
- partial weigth of the embankment loading the soft soil, considering only the loads that will actually load the soft soil. This weight was estimated using Raithel´s analytical method. In this scenario, soft soil shear strength was considered without the improved shear strength due to the sand columns.

Usually, the contribution of the sand column as vertical drains is not considered in this design approach. The average shear strength parameters are increased due to the vertical loads in the granular material. A careful parametric verification is necessary, considering sets of deformability and shear strength parameters. Artificially low shear strength of the soft soil can generate artificially high loads in the sand columns.

Design established strict necessity of monitoring with instrumentation. Figure 2.19 shows the position of the instruments in the section, including perfilometers to measure continuous settlement, measurement of in-depth horizontal displacements with inclinometers (IN-A and IN-B, installed before construction of the columns), load cells to monitor stress at the top of GECs and measurement of diameter change of GEC with crackmeters placed in orthogonal directions (see details of positioning of load cells and crackmeters in figure 2.20). The main data obtained with the instrumentation for the section under scrutiny is shown in figures 2.21 to 2.26.

Other aspects of the design as well as the results of geotechnical tests have been described previously (de Mello and others, 2002, 2008a and 2008b). Figure 2.19 presents the design section, chainage 1133.

At the onset of construction, due to the very soft superficial soil, a work platform was built to allow operation of equipment (see figure 2.19). During construction, it was necessary to thicken the platform to some 2 to 3 meters to avoid flooding by an adjacent river. A photograph of the job is shown in figure 2.27. Information from job engineers indicate that "raising" of the platform was felt (but, unfortunately, not measured) during construction of the GECs. Spoiled sand, used to fill the GECs, may also have contributed, to a lesser extent, in increasing the thickness of the platform.

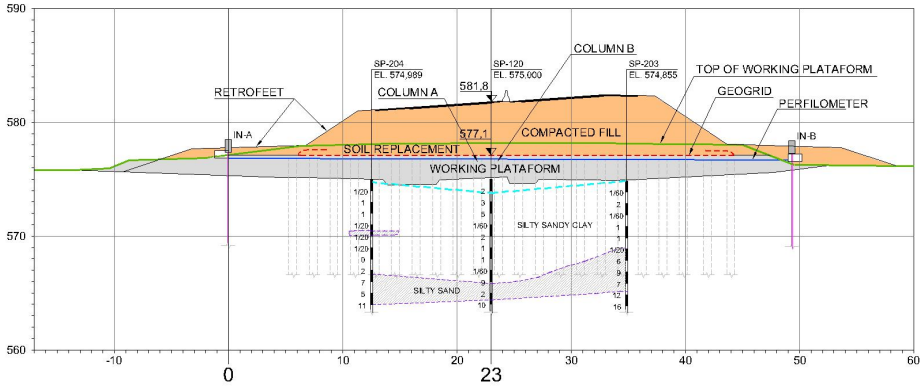

Figure 2.19. Fill section and position of the instruments

Inclinometers have been installed before the placement of the GECs, some 4 to 5 meters apart from the positions where the 70-cm closed-end steel tubes were driven. This allowed observation of horizontal displacements during construction of the GECs in both sides of the future fill, which, as can be seen in figures 2.23 and 2.24, were quite different: while inclinometer IN-A showed less than 1 cm of displacement, restricted to the top 3 or 4 meters, inclinometer IN-B displaced some 15 cm at the surface and showed displacements varying "linearly" to a depth around 10 meters. Apparently the wider working platform, that existed at the position of inclinometer IN-A (see figure 2.19), helped in reducing the horizontal displacements.

Raithel's method has been used for estimating stresses, deformations and settlements in two occa-

sions: end of construction (December 2006) and 28 months after start of operation of the road (April 2009). The geotechnical parameters used in such back analyses are shown in figure 2.28. The work platform has been taken into consideration.

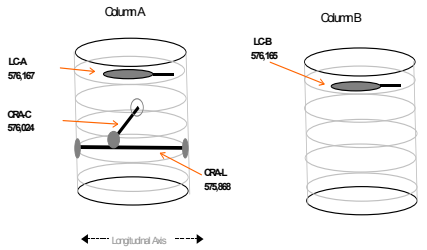

Figure 2.20. Load cells and crackmeters in GECs

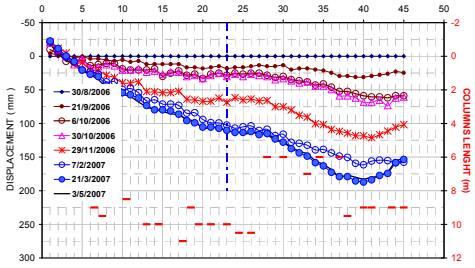

Figure 2.21. Settlements – Cross section

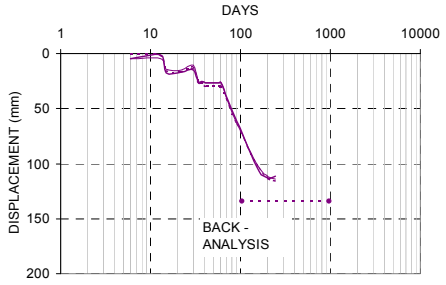

Figure 2.22. Settlements – Road axis

For end of construction, the average initial strength of the soft soil has been used (see figure 2.28). The rigidity of the geotextile has been taken from the quality control tests. Main results were as follows:

- Estimated vertical stress at the load cells position resulted equal to 273kPa, to be compared with measured values of 110 kPa (LC-A) and 210kPa (LC-B), see figure 2.25;
- Calculated radial deformation was 0,9mm (same in all directions, according to the calculation method), against measured values around 0,10 mm (CRA-C, transversal direction) and 0,50 mm (CRA-L, longitudinal direction), figure 2.26 shows diametric deformations;
- Settlement at the road axis have been estimated as 13,3cm, in opposition to measured values of the order of 8 to 9 cm, figure 2.22

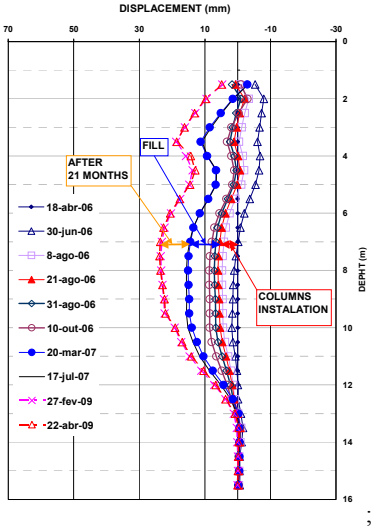

Figure 2.23. Inclinometer A - Transversal direction (displacements in the longitudinal direction less than 1 cm)

Calculations for end of construction indicate that the vertical load at the top of the work platform is distributed roughly 50% in the columns and 50% in the fill. At the top of the soft soil, 80% of the vertical load goes to the columns.

For the 2009 data, 28 months after start of operation, the geotechnical conditionings have been reviewed. The geotextile rigidity has been reduced in accordance with the creep curve of PVA (J = 2100 kN/m), the increase in undrained strength has been considered (Mesri, 1975) and compatibility with end of construction displacements has been maintained. Main results were as follows:

- Estimated vertical stress at the load cells position reduced to 260kPa, to be compared with measured values of 150 kPa (LC-A) and 235 kPa (LC-B), see figure 2.25;
- Calculated radial deformation increased to 0,95 mm, against measured values of 0,40 mm (CRA-C, transversal direction) to 0,95 mm (CRA-L, longitudinal direction), figure 2.26;
- Estimated settlement at the road axis kept at 13,3cm, while the measured value increased to 11,5 cm, figure 2.22**.** It is to be noted (figure 2.22) that in march 2007 the settlements had already reached their final value, a beha-

vior to be expected from the vertical drain action of the GECs.

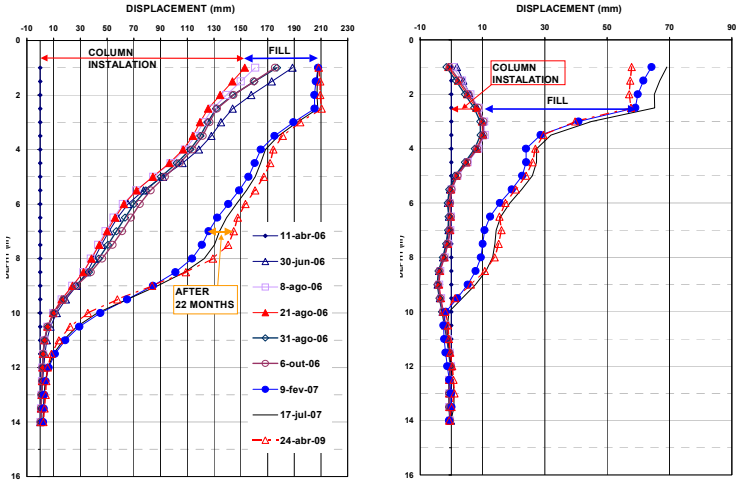

(a) (b)

Figure 2.24 Inclinometer B – (a) Transversal direction; (b) Longitudinal direction

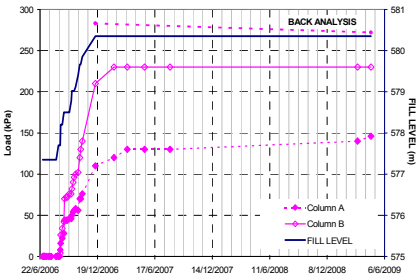

Figure 2.25. Results from load cell

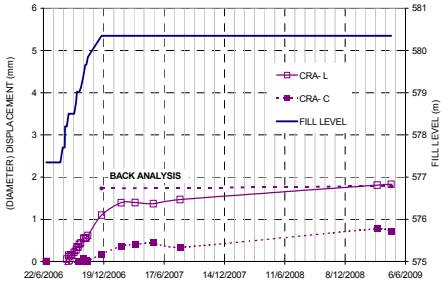

Figure 2.26. Crackmeter results

Figure 2.27. Photograph of the site during construction

COMPRESSIBILITY

Soil	Original Design (2000) OCR	CR	RR	cα	Revised Design (2006) OCR	CR	RR	cα
Black to dark gray organic silt clay (soil C)	1,2	0,40	0,025	0,03	1,0	0,25	0,04	0,02
Gray silty sandy clay (soil B)	1,2	0,10	0,02	0,03	1,1	0,25	0,04	0,02
Gray caly silt sand (soli A)	1,2	0,10	0,02	0,03	1.1	0,10	0,02	0,02

CONSOLIDATION COEFFICIENTS

Soil	Original Design (2000)	During Construction	Phase II (2006)
Black to dark gray organic silt clay (soil C) Gray silty sandy clay (soil B) Gray clay silt sand (soil A)	1 x10^{-7}	3.8 to 4.4 x 10^{-7}	2 x10^{-7}

SHEAR STRENGTH

Soil	Original Design (2000)	Revised Design (2006)
Black to dark gray organic silt clay (soil C) Gray silty sandy clay (soil B) Gray caly silt sand (soli A)	10+0,94z	6kPa (z=2m) 6+z (z>2m)

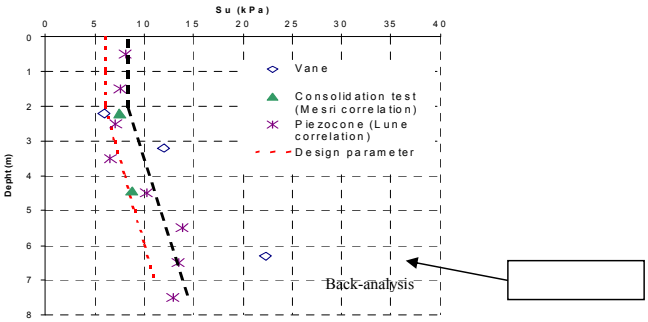

Figure 2.28. Parameters GEC road fill

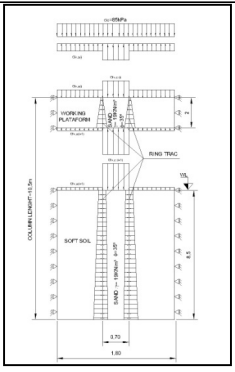

Scenario 1: End of construccion

Material	γ(kN/m^3)	cohesion(kPa)	ϕ	Eoed (kPa)	ν
Working plataform	17	10	25	8100 a 10750	0,25
Soft soil	15	s_u=7,5+z	0	880 a 1425	0,4

Scenario 2: 28 Months of Operation

Material	γ(kN/m^3)	cohesion(kPa)	ϕ	Eoed (kPa)	ν
Working plataform	17	10	25	8280 a 10900	0,25
Soft soil	15	s_u=0,22(σ_{vs}+$\sigma_{vs,diff}$)	0	1365 a 1890	0,4

Results of Back-analysis	Scenario 1 σvs(kPa)	σvc(kPa)	Scenário 2 σvs(kPa)	σvc(kPa)
Top of column	49	109	52	104
Top of soft soil	19	175	29	153

Figure 2.29. Parameters for back analysis - GEC ROAD FILL

The share of load at the columns, calculated for the "long range" situation, reduced to about 70%.

The comparisons indicate, in general terms, for the present case, that the displacements calculated for the construction stage tend to be smaller than the measured ones. On the other hand, for the "long range" situation the calculated values are similar to the field values. This coincidence is to a certain extent surprising given the uncertainties and inexactitudes of the method, particularly in what concerns the remoulding of the soft soil whose deformability has a strong influence in the results.

The horizontal displacements associated with fill construction were around 5 cm to 6 cm and were similar in both sides of the fill (see figures 2.23 and 2.24). Comparing the vertical volume of displacement, Vv (which can be obtained from figure 2.21) with the horizontal volume of displacement, Vh (obtained from figures 2.23 and 2.24), it can be verified that the relation Vv/Vh remained above 7 which, as suggested by Sandroni, Lacerda & Brandt (2004), indicates that safety against a slip failure has been comfortably kept at distance.

2.4.4 Case 2: GECs under fill for coal stacker rails on soft clay

GECs, 8 to 9 m deep, with 0,78 m diameter, in a 2 m square array, have been used under a fill reinforced with geogrids. On top of the fill, ballast, sleepers and rails for a coal stacking machine have been built, as shown in figure 2.30.

The original soil profile at this site showed, from top to bottom, a 6 to 7-meter thick soft organic clay with piezocone q_c less than 500 kPa, followed by a 2-meter thick clayey sand layer, then a 4 to 6-meter thick organic clay with q_c above 1.000 kPa and, finally, denser, more competent sedimentary sandy layers. The bottom of the GECs is at the clayey sand layer.

Figure 2.30- Stacking machine fill on GECs

Upon construction of the fill, ballast and sleepers, settlement of a few centimeters has been observed (as opposed to some 20 or 30 cm that would happen without GECs). A load test with the stacker machine showed the following settlements:

- Upon 20 passages of the machine, 2 to 3 cm of settlement happened;
- With the machine standing at a single position during one week, a further settlement around 2 cm has been measured

3 GEOSYNTHETICS AND MINING RESIDUES IN GEOTECHNICAL APPLICATIONS

3.1 *Introduction*

Due to their characteristics of versatility, low cost and constructive easiness, geosynthetic materials have become basic components in the design and performance of mining facilities. At mine sites, geomembranes have been primarily used as base liners for heap leach and liquid containment systems (drainage waters, treatment ponds), and to some extent, for tailings and other solid waste storage structures. Geogrids and geotextiles have been used to stabilize soft soils and slopes or to provide additional storage capacity. Geotubes have been used for the conveyance of runoff, drainage, and process waters, and/or for leak-detection systems.

On the other hand, the mining activity generates a huge amount of different types of residue and some of the sub-products from the ore treatment processes may present satisfactory mechanical properties for usage in geotechnical works. The combination of the mining residues (wastes or tailings) with geosynthetic reinforcement may provide a cheaper, technically feasible alternative as opposed to the use of more expensive construction materials.

Waste consists of a material (soil or rock) that does not contain commercially attractive amounts of precious metals and is usually disposed off in piles. Tailings are the remaining products of ore processing, with their physical and mechanical properties depending on the type of ore (iron, bauxite, gold, etc.) and on the process of treatment, grading from fine sand to slimes. Depending on the processing method, these materials can be active (contaminated) or inert (not contaminated).

Tailings are generally transported as solid-water mixtures, called slurries, and deposited by hydraulic techniques. For their final disposition, the mining companies have used the tailings themselves as construction material for dams. These disposition procedures often produce tailings deposits with a high void ratio. In addition, such sediments undergo a complex process of natural particle segregation as a consequence of the different densities of the existing minerals. This is particularly important for tailings deposits of iron ore because of the random interaction effects of different silica and iron oxide particles of different grain size.

Brazil has a privileged position in the rank of worldwide reserves and is the most important miner-

al producer in Latin America. Brazil has a diversified mineral production and is the largest exporter of iron ore and niobium alloys. It is also one of the major producers of niobium, iron, kaolin, tantalite, bauxite, graphite, cassiterite, vermiculite, ornamental rocks, talc, phosphate rock and gold.

Brazil has several mining provinces but the most important of them is the so-called *Quadrilátero Ferrífero* (Iron Quadrangle) region. This special area (QF) is located in the State of *Minas Gerais*, southeastern Brazil, corresponding to an area of about 7,000 km^2. This region is known for its immense deposits of iron ore, gold, manganese, and several other valuable minerals, which are mined by several industries, from large conglomerates up to countless small-to-medium-sized mining companies.

The intense exploitation during the last decades in this region has produced a considerable amount of tailings that have to be properly disposed of during the mining operation. At the same time, there is an increase in the requirements for environmental protection including new standards. So an adequate mining management policy should include a reduction in the volume of surface waste and some potential applications for the generated residues. In this context, the use of synthetic materials has gained increasing attention in mining projects. Some recent Brazilian applications and research (predominantly in the QF region) are presented in the subsequent topics, including geotechnical applications using mining residues - geosynthetics as composite material (Cases 2 to 6) and an example of use of geosynthetics for increasing the storage capacity of tailings disposal systems (Case 1).

CASE 1: REINFORCED WALLS FOR TAILINGS STORAGE SYSTEMS (Costa Filho & Sieira, 2008)

Geosynthetic reinforced walls or slopes have been commonly used in Brazil in projects for increasing storage capacity and for closing of tailings disposal systems. These structures are designed associating soils and synthetic inclusions (geotextiles and geogrids) for restricting excessively long earth fills.

Costa Filho & Sieira (2008) presented some recent examples of such applications for increasing the storage capacity of tailings disposal areas. The first example reviewed here refers to a bauxite residue disposal area located in the State of Minas Gerais. The disposal systems have been built using perimeter compacted earth fills as containment dykes, with internal slopes of 2.5H:1V and external slopes of 2.0H:1V. A single composite sealing system, consisting of a 0.8mm thick PVC geomembrane, over a 50cm thick compacted clay layer, covers the bottom and the slopes of the pond. The residue has high alkalinity (pH $\cong$ 12) and contains heavy metals. The adopted solution involved the construction of a reinforced soil wall in the upper part of the perimeter dykes (Figure 3.1).

The total length of the upper dykes is 1710m, with a constant height of 5.0m and nine layers of PVC geogrids as reinforcing elements (with a nominal strength of 55kN/m on the 6 bottom layers and of 35kN/m on the 3 upper ones). The external face was protected with bags of organic soil with seeds, wrapped by the geogrids, and by an erosion control mattress covering the whole face.

The structure was built in two stages due to the large earthmoving volumes of the perimeter dykes and the relatively short dry period in the region (Costa Filho *et al*., 2006). In the beginning the productivity was in the order of 115m^3 of reinforced fill per day, reaching 260 m^3/day throughout the subsequent stages, with peaks of 300m^3/day. Small movements were observed during construction, in the order of 25 to 50 mm at a height of about 2.0m, representing a maximum horizontal average strain of 1.25% (Becker, 2005).

Nowadays, the disposal area is almost completely full of residue and the reinforced wall presents no signs of excessive movements. Maximum values for horizontal displacements are in the order of 7.6 cm at the top of the wall and the maximum crest settlement is around 6.0 cm.This good behavior is related to the great stiffness of the geogrids and to the quality control procedures applied during construction.

A second similar example refers to a tailings deposit (Figure 3.2a) that has a solid content of about 10-15% and contains a significant amount of metals, particularly zinc, cadmium, lead and iron. For this reason the deposit is lined with double PVC geomembranes associated to a leak collection by an overlain base drainage layer.

The project presented several conditional features: the reservoir is located in a closed valley; the foundation is typified by very soft alluvial deposits of clay and peat materials; system closure was delayed to permit additional tailings storage and this necessity imposed the extension of the reservoir impermeabilization to the new internal slope and on the existing crest width of 5.0m (Costa Filho & Sieira, 2008). The adopted solution consisted of a geosynthetic reinforced wall with 2.0m in height and about 250m in extension along the crest (Figure 3.2b) for attending approximately 1 year of residue storage demand. A non-woven geotextile of continuous filaments of polyester (tensile strength of 21 kN/m and mass per unit area of 300 g/m^2) was used as the reinforcing element of a compacted silt-clayey soil. The geotextiles were spaced 30cm for the entire width of the crest and wrapped around both slopes.

The PVC geomembrane was extended on the upstream slope, welded to the existing geotextile, anchored at the crest, and protected by a non-woven geotextile impregnated with mortar. The downstream slope protection consisted of a shotcrete layer

about 5cm thick, with a light steel reinforcement mesh. Maximum differential settlements in the order of 20cm were observed in the longitudinal direction and horizontal displacements of the external slope were also very small; results that have ratified the good performance of the reinforced wall.

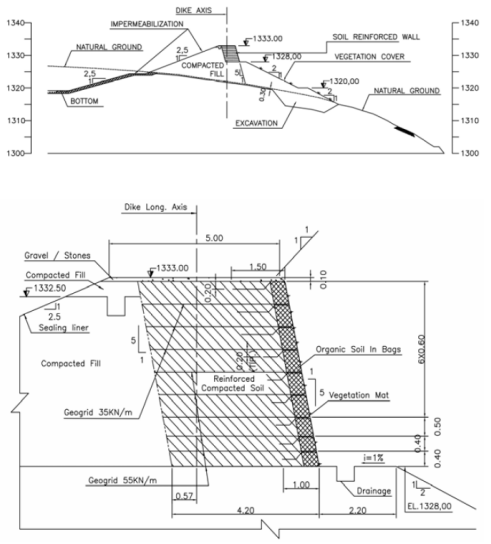

Figure 3.1. Cross section of the perimeter earth fills and of the upper reinforced dykes (Costa Filho & Sieira, 2008)

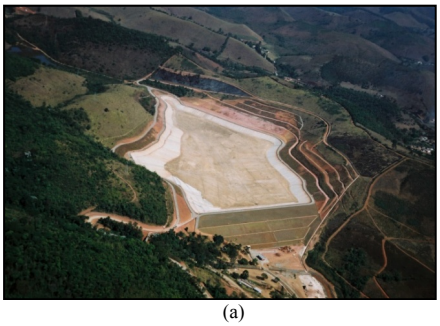

(a)

(b)

Figure 3.2. Zinc tailings disposal system. (a) general view of the deposit; (b) upstream and downstream slope views (Costa Filho & Sieira, 2008)

CASE 2: REINFORCED SLOPE AT THE BR 381 HIGHWAY (Gomes & Martins, 2003)

A solution, similar to that of case 1, involving mining residues instead of local soils has been applied for BR 381 highway slope stabilization located in the *Quadrilátero Ferrífero* region. In a place known as *Variante da Ingá*, located at km 463.24 of Federal Highway BR 381, stands one of the largest reinforced soil slopes already constructed in South America, 18m in height and 270m in extension. This structure was characterized by nonconventional features in terms of dimensions, nature of the materials and low strength of reinforcement elements (Gomes & Martins, 2002).

In the critical zone of this slope, situated between stations 20+15.00 and 24 +15.00, the reinforced structure reaches 18.0 m in height and was predesigned in three sections, 6.0 m high each (Table 3.1) with slopes of 1H:2V and berms 3.0 m wide, based on the application of conventional soils and using characteristic values from similar places and materials. A conventional embankment, 10.00 m in height and with inclination 3H:2V, overlaps the reinforced structure (Figure 3.3).

Table3.1. Basic geometry of the reinforced slope of the BR 381

walls	height (m)	Sections (m)	layers	spacing (m)	length (m)
A	6.0	0,0 - 6.0	30	0.20	3.60
B	6.0	6.0 – 12.0	15	0.40	6.20
C	6.0	12.0 – 18.0	15	0.40	6.20

The original design of the slope was modified in order to overcome the difficulties to obtain granular soils in the area and due to the availability of large residue volumes from an iron ore mine situated in the vicinities. Laboratory investigations on these residues demonstrated their satisfactory mechanical properties for usage in composition with geosynthetics in the reinforced slope structure.

Two different types of residues were used (Table 3.2): wastes in the execution of the lower section and, on a greater scale, iron ore tailings for the intermediate and upper sections. The replacement of wastes for ore tailings in a large part of the reinforced slope was done due to limited amount of this material produced from mining activities

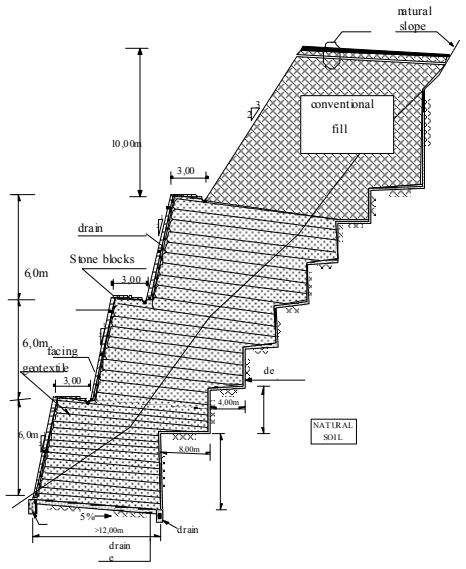

Figure 3.3. Typical section between 20+15.00 and 24+15.00 stations (Gomes & Martins, 2003)

Table 3.2. Physical parameters of the residues

physical parameters	waste	tailings
G_s	3.59	4.22
% gravel* % sand* % silt* % clay*	36.7 25.5 17.8 20.0	35.1 36.3 26.4 2.2
w_L , I_P (%)	44 , 17	NP
$\gamma_{d\,max}$ (kN/m^3)	22..3	26.2
e_{max} , e_{min}	-	0.89 , 0.58

* ABNT - Brazilian Standards

The potential for using these materials in reinforced slopes was analyzed for two different reinforcements: nonwoven geotextiles of polyester, with tensile strength of 40kN/m and woven geotextiles of polypropylene), with tensile strength of 75kN/m.

Specific tests were carried out to assess the mechanical interaction among the materials used in the real structure. The interface strength parameters are given in Table 3.3 and the effects of the confining pressures on the tensile behavior of the geotextiles are presented in Figure 3.4. Based on these results, the structure was recalculated and the arrangement obtained for the lower section consisted of 08 layers of woven geotextiles, each one being 4.85m in length and with a spacing from 0.40m to 0,80m. The corresponding demand of geotextiles was about 57.60 m^2/m (a reduction factor of 64.4% in relation to the original conception), with an overall factor of safety against rupture of 1.75.

The intermediate and the upper sections were designed to behave only as a medium slope. The arrangement presented 16 layers of nonwoven geotextiles, with 4.50m in length and a spacing between 0.40m and 0.80m, for a demand of 109.60 m^2/m (reduction factor of 55,4% in relation to the original conception) and an overall factor of safety of 1.52. The face consisted of a rip-rap system, using cement-soil bags and the drainage system was projected as a 20 cm thick layer.

Table 3.3: Interface strength parameters for the materials of the reinforced slope of the BR 381

interfaces	soil		interface		Coefficients	
	c' kPa	ϕ' (^{o})	c_g kPa	ϕ_g (^{o})	a	F
Waste[1]	13.1	48.3	-	-	-	-
waste/wG[2]	-	-	13.4	28.7	1.02	0.49
Tailings[1]	16.7	42.7	-	-	-	-
tail./nwG[2]	-	-	9.5	42.5	0.57	0.99

[1] soil conditions at natural moisture content
[2] wG: woven geotextile;
nwG: nonwoven geotextile.

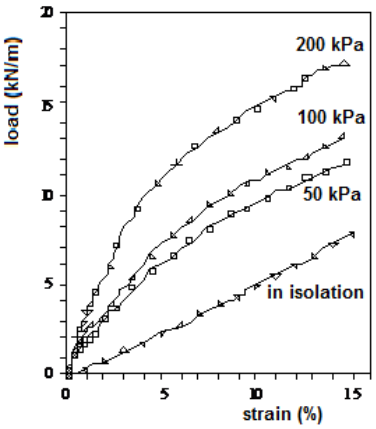

Figure 3.4. Effects of the confining pressures on the tensile behavior of the geotextiles (Gomes & Martins, 2003)

The demand of the geotextiles represented 53% of the total cost of the designed structure value reduced to 51% with the performed structure (Figure 3.5). It comprised amounts of 21,360 m^2 of woven geotextiles and 72,500 m^2 of nonwoven geotextiles used in the structure.

The overall behavior of the walls was adequate, with no records of local instabilities and severe or atypical movements. The monitoring of the wall during construction and along its initial period of operation indicates displacements and settlements limited to the foreseeable ranges, with a tendency for stabilization. Design and construction of other reinforced soil structures using geosynthetics and mining resi-

dues have been implemented in highway embankments and bridge abutments in the QF region. These projects clearly demonstrate the potential of this technique and the significant contribution of using local materials, particularly residual soils and mining residues, to reduce the overall costs of such structures.

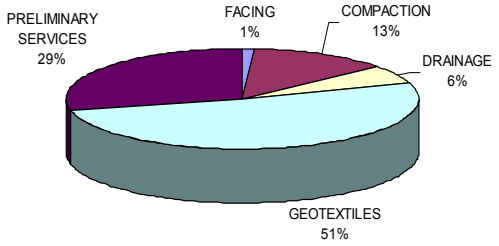

Figure 3.5. Cost distribution for the performed structure (Gomes & Martins, 2003)

CASE 3: GEOSYNTHETICS AND MINING RESIDUE APPLICATIONS FOR PAVEMENT INFRASTRUCTURES (Saraiva, 2006; Gomes & Saraiva, 2010)

Research projects have been conducted in Brazil to quantify the potential benefits of including geosynthetics in pavement layers. These approaches range from a passive use of materials, creating a separation between pavement layers, up to active reinforcement inclusions able to stand self-weight and surcharges due to heavy traffic. In a few cases, field instrumentation has been used as support methodology to obtain the operational and critical pavement responses in terms of strains, pressures, temperatures and moisture contents.

In Brazil such research has been implemented in the *Quadrilátero Ferrífero* region to determine how and under what conditions geosynthetics (geogrids and geotextiles) increase the structural capacity of pavements designed with iron ore mining residues as construction material. Field tests comprised the construction of full-scale pavement test sections, where various configurations were used and submitted to actual traffic conditions under continuous monitoring.

The experimental program was carried out in a 300 m segment of a secondary road that connects the cities of *Itabira* and *Senhora do Carmo* in the State of *Minas Gerais*. Although the road is addressed for conventional traffic, the test segment constitutes a short strip primarily used for transporting iron ore in big trucks. This experimental segment was subdivided into six sections of 50 m each (Figure 3.6).

To construct the instrumented pavement test sections, initial soil and mining residue sampling was performed at different points and tested under various proportions aiming to define an adequate mixture for a base material, according to standards dictated by the Transport Department of the State of *Minas Gerais*.

Laboratory investigations included characterization tests, soil characteristic curve tests, CBR tests and chemical analyses (Saraiva, 2006). Six instrumented flexible pavement test sections, 50 m long each, were built to examine the effects of geogrid and geotextile reinforcement. All sections present the same course thicknesses: 20 cm for subgrade, 15 cm for subbase and 18 cm for base, with hot-mix asphalt thickness averaging 6 cm. The base material consisted of ore gravel with a CBR value of 89.7% (adopted in section 1 according to the project) or was composed of an optimized mixture of iron mining residues (70% waste and 10% fine tailings) collected directly from their respective disposal systems and the subgrade local soil (clay with a CBR value of 7%, 10% in weight). Another kind of mine gravel (with CBR varying between 45.0% and 67.8%) was adopted as subbase material in all test sections. Geosynthetic stabilization (Figure 3.7) was placed on top of the base layer (a non woven geotextile in Section 3 and a biaxial geogrid in Section 4) and on the bottom of this course (non woven geotextile in Section 5 and geogrid in Section 6), while Section 2 was not stabilized.

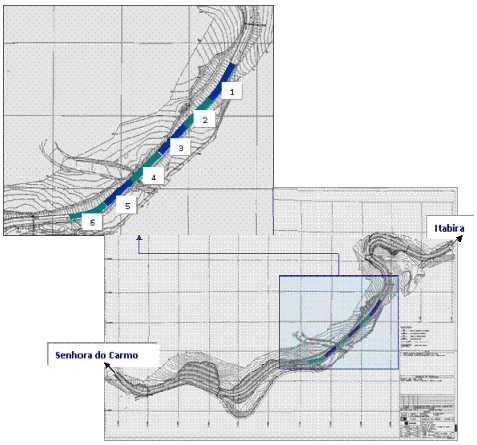

Figure 3.6. 300m segment and test sections (Gomes & Saraiva, 2010)

The pavement test sections were instrumented with strain gauges (positioned in parallel and perpendicularly to the pavement surface), thermocouples, and soil moisture cells. The deformation gauges were 10 cm long and consisted of extensible electric resistances (strain gauges) fixed to circular resin plates at the ends and previously mounted and

calibrated in the laboratory (Figure 3.8). In addition, temperature and moisture content gauges (*CS615 Water Content Reflectometer*) were also installed in all courses of the test sections. An extensive instrumentation infrastructure was constructed to locate all underground instrumentation, cables, and data acquisition facilities. In addition, data acquisition systems and signal processing programs were developed specially for this research.

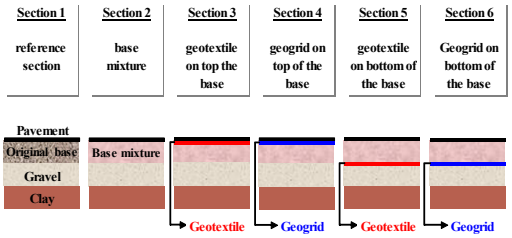

Figure 3.7. Pavement test sections (Gomes & Saraiva, 2010).

Instrumentation data were complemented with Benkelman beam tests performed on the test sections at different times during the experiments. For these tests a loaded truck with 82kN on a single axle with dual tires inflated to 560kPa was employed. Measurements were made by placing the tip of the beam between the dual tires and measuring the pavement surface rebound as the truck moves away. In addition, for construction control, in-situ density sand cone and in-situ stiffness tests were performed. The latter consists of determining soil stiffness from its dynamic response using a geogauge H4140 apparatus. This device estimates in-situ stiffness based on the successive measurements of ground surface displacements caused by the application of a constant cyclic compressive load.

Figure 3.9 shows results of maximum surface deflections obtained in Benkelman beam tests performed on the course pavement materials. A larger variability of the results occurred for the subgrade and subbase material probably as consequence of the greater heterogeneity of their geotechnical properties. Geosynthetic stabilization effects are clear regarding an expressive reduction and regularization of all deflection values when the inclusions were inserted on the bottom of the base layer

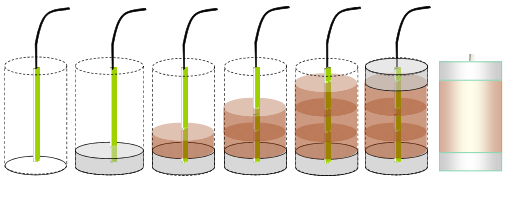

(a)

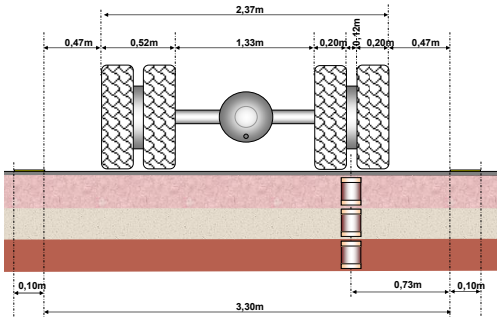

(b)

Figure 3.8. Pavement instrumentation: (a) deformation gauge assemblage; (b) vertical deformation gauge installation (Gomes & Saraiva, 2010)

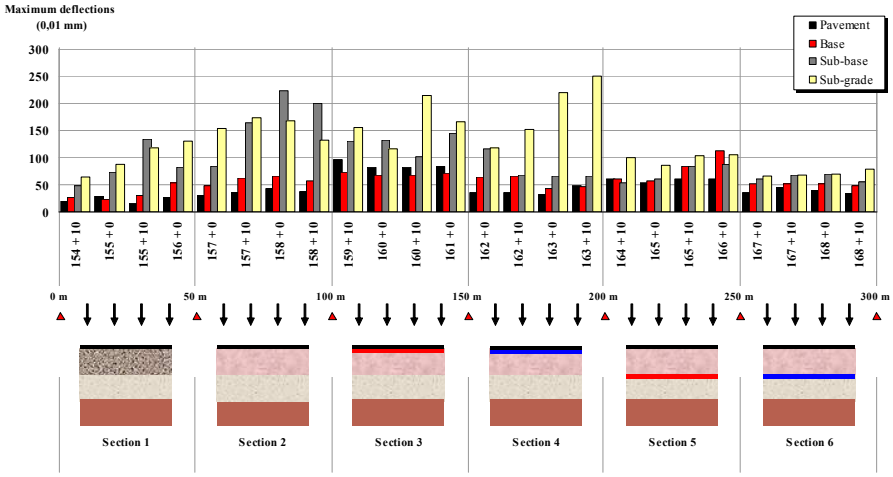

Figure 3.9. Maximum surface deflections obtained in Benkelman beam tests (Gomes & Saraiva, 2010).

Figure 3.10 shows the average values of the vertical displacements obtained for each section and for each course. It can be seen that the maximum deflections values for subgrade were larger than the limit value of 1.20 mm, recommended by the Transport Department of the State of *Minas Gerais*, with the exception of Section S1 (reference session) and Section 6 (reinforced section with geogrid at the bottom of the base layer). On the other hand, for duplication works of the Federal Highway *BR 381* cited previously, the vertical displacements measured in the subgrade course varied between 0.86 mm and 1.44 mm. In this range perspective, deflections showed to be incompatible only for the sections with the geosynthetic reinforcement positioned on top of the base layer (Sections 3 and 4).

Similarly, Figure 3.11 shows the average values of the stiffness obtained by the geogauge apparatus for each section and for each course. A smaller value was obtained for Section 3 (geotextile on top of the base layer). Such condition propitiated a sensible reduction of the asphalt stiffness by the effects of the geogauge vibration absorption due to the inclusion of a non-woven geotextile practically on the pavement surface.

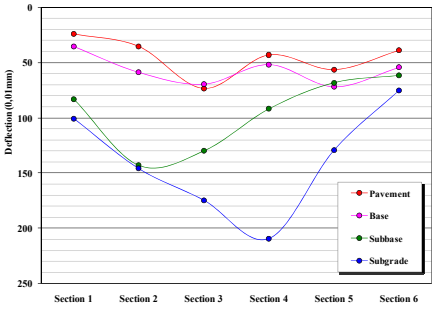

Figure 3.10: Average values of the deflections for each section and for each course (Gomes & Saraiva, 2010).

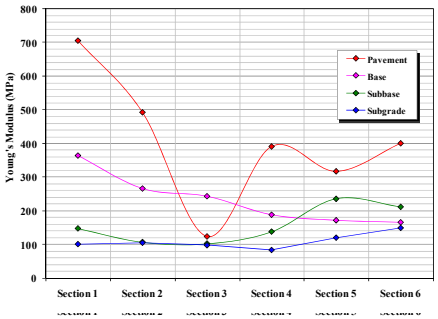

Figure 3.11. Average values of the material stiffness for each section and for each course (Gomes & Saraiva, 2010).

Instrument survivability for the strain gauges has ranged from 75 percent after 100 days to 0 percent after 293 days of operation. The majority of instrument failures occurred after six months of operation. All gauges were exhumed and submitted to detailed analyses to characterize and to quantify the potential problem sources (Gomes & Saraiva, 2010).

CASE 4: GEOSYNTHETIC AND MINING RESIDUE APPLICATIONS FOR HEAVY LOAD RAILWAY MITIGATION (Fernandes, 2005; Fernandes, Palmeira & Gomes, 2008)

Most of the railroad system in the State of *Minas Gerais* is directed to mining activities and primarily for ore transportation. In this context, due to heavy and cyclic loading, railway ballast breaks down and deteriorates progressively under train cyclic loading, resulting in great settlements and rail distortions. Because of this, good and expensive ballast materials are required in railway construction and maintenance. In an attempt to solve such problems, an extensive research and monitoring program was conducted to verify the potential application of mining residues and geosynthetics for improving the deformation characteristics of railways, with emphasis on the substitution of part of the good quality subballast material by a mixture combining mining waste and geosynthetic reinforcement. For this study, a number of experimental sections were constructed and instrumented, according to the same concept and methodology presented in the prior case study.

The experimental program was carried out in a segment of the *Vitoria-Minas* railway, in the State of *Minas Gerais*. The railway is 104 years old, 898 km long and is responsible for approximately 40% of the load transported by railways in Brazil. The daily traffic is very intense, imposed by approximately 16 compositions (2 locomotives of 160 tonnes plus 100 wagons of approximately 100 tonnes each – 300 kN axle load). The steel sleepers are of the type UIC865, with dimensions of 2.2 m x 0.3 m x 0.02 m. The rail type is TR 68. Figure 3.12 presents the geometric characteristics of a typical railway cross section and the experimental test section arrangements (sections S1 to S6, 250m long each), with different types and location of geosynthetic materials. All sections were composed of 450 mm of ballast and 200 mm of subballast.

In sections 2 to 6 an alternative subballast material was employed replacing the traditional aggregate used for subballast in Section 1 (reference section). The alternative subballast material consists of a mixture of the subgrade local soil (silty sand, average particle diameter of 0.13mm, 50% in weight), a fine mine waste (sandy silt, average particle diameter of 0.032mm, 25% in weight) and the traditional

subballast material used in Section 1 (sandy gravel, average particle diameter of 5.1mm, 25% in weight). The same ballast material (a kind of steel slag) was used in all test sections. A non-woven geotextile of continuous polyester filaments (mass per unit area of 300 g/m^2) and a biaxial geogrid, also made of polyester fibers with a HDPE cover, were used in test sections 2 to 5.

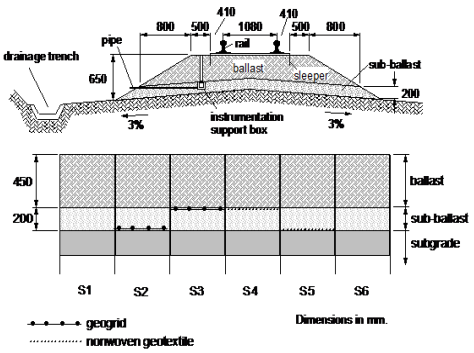

Figure 3.12. Typical railway cross section and experimental section arrangements (Fernandes *et al*., 2008)

Monitoring of the sections on the railway segment (Figure 3.13a) included soil deformation gauges at the top and bottom of the ballast material (Figure 3.13b), temperature and moisture content gauges and rain gauge meters. Gauges were calibrated and checked before installation and the data acquisition was obtained under real in-service conditions of the railway, typified by a continuous and heavy traffic. On the other hand, duplication of gauges permitted researchers to check the quality of the data.

Benkelman beam tests were carried out on the test sections at different times during the experiments (Figure 3.13b). For these tests a locomotive weighing 1600 kN with 200 kN/axle was employed. Additional information on the materials and methodology used is reported by Fernandes (2005).

Figure 3.14 shows the variation of horizontal strains at the bottom of the subballast layer with the number of train axles that passed on sections S1, S3, S4 and S6. The measurements were made under the sleeper and on the vertical passing of the rail center line. For 600,000 passages of train axles, the performance of all sections was similar. After that, sections S3 and S4 presented less horizontal strains than the reference section S1. Section S6 (unreinforced alternative subballast material) was the one that presented the highest horizontal strains at the base of the subballast layer.

(a)

(b)

Figure 3.13. Vitoria-Minas railway. (a) General view of the segment test; (b) Benkelman beam tests and installation of deformation gauges in the track (Fernandes *et al*., 2009).

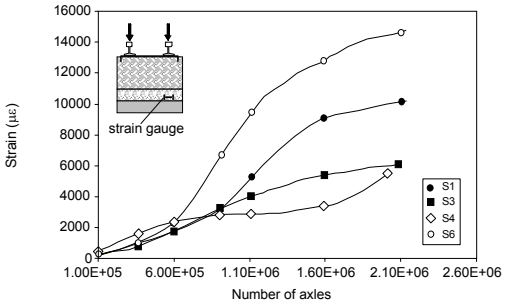

Figure 3.14. Horizontal strains at the bottom of the subballast (Fernandes *et al*., 2008).

Figure 3.15 presents the variation of vertical strains at the base of the subballast layer with the number of train axles. Not much difference in results is observed up to 100,000 train axles. As train traffic increases, section S6 tends to present the largest vertical strains, followed by section S1, although the latter shows signs of reduction on the rate of strain with traffic intensity. The same trend of reduction of the rate of strain with the number of train axles is observed for section S3 after the passage of 1,500,000 train axles.

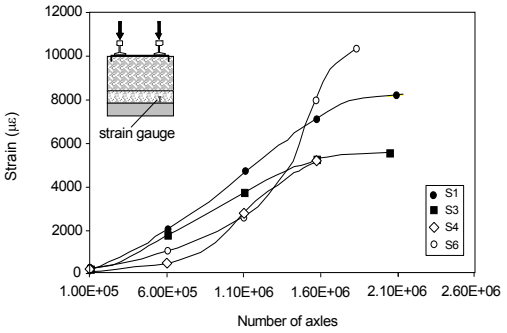

Figure 3.15. Vertical strains at the bottom of the subballast (Fernandes *et al*., 2008).

Ballast samples from the test sections were collected for testing during the monitoring period. Grain size distribution analyses and Los Angeles abrasion tests were conducted on the ballast samples. Figure 3.16 shows results of the grain size distribution analyses after 600 days of monitoring, corresponding to a passage of 2,120,000 train axles or 75,860,070 tons on the test sections. The grain size distribution of the ballast material before traffic is also shown for comparison. In comparison with the ballast grain size distribution curve before traffic the results obtained for sections S1 and S6 were the poorest. Among the reinforced sections, section S2 (geogrid at the sub ballast base) was the one presenting the greatest grain size reduction.

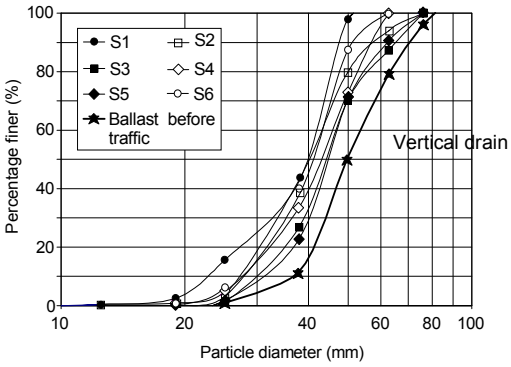

Figure 3.16. Grain size distribution curves of the ballast material after 600 days of traffic (Fernandes *et al*., 2008).

The field results showed that the geosynthetic reinforcement reduced the compressibility of the system composed of mining waste. Less breakage of the ballast material and greater abrasion resistance were observed in the test sections with geosynthetic inclusions. This proposed application can be very attractive to the mining industry in situations where reasonably good quality mining waste is plentiful and conventional track construction materials are scarce or expensive.

CASE 5: DRAINAGE AND FILTRATION SYSTEMS OF TAILINGS DISPOSAL AREAS (Araújo, Gomes & Gardoni, 2007; Palmeira, Beirigo & Gardoni, 2009)

Conventional tailings disposal methods and storage facilities (in contraposition to contaminant disposal systems shown in Case 1) include slurry disposal at a valley storage (tailings discharge downstream towards a water retaining containment wall where they decant to collect the supernatant water is located, or upstream away from the containment wall with a decant facility located at the upstream end) and slurry disposal on a series of cells. The tailings are deposited by cycling along the cells to facilitate the consolidation and desiccation processes.

Although geosynthetics have been extensively used as drainage and filtration elements in various geotechnical works, concerns still persist regarding their long-term behavior in waste disposal systems. The main issues for the use of geosynthetic drainage systems in such works are as follows: possible short or long-term clogging of the synthetic filter, filter retention capability, effect of high stress levels on the geosynthetic hydraulic characteristics, and biological clogging in waste disposal drainage systems.

Figure 3.17 shows a typical drainage system used in drying cells for dewatering of fine grained tailings slurry, with an initial concentration of solids between 25% and 35%, consisting of wells made of gabions enveloped by a nonwoven geotextile.

Figure 3.17. Typical drainage system in drying bay (Palmeira *et al*., 2009)

In general the deposition area is located in a valley not far from the plant and the tailings are confined laterally by the valley sides and longitudinally by dykes, which divide the total area into storage basins (each side with some hundred meters). Dumping is

cyclic; each basin is used for a short period (10 days for example) then allowed to rest for another period (30 days for example) before repeating the cycle. During the resting time, the tailings consolidate and dry to reach solids a content of 70 to 80%, at which point they should be stable and occupy their minimum volume.To investigate the effective performance of nonwoven geotextile filters in contact with tailings, different combinations of interfaces have been submitted to compatibility tests in the laboratory, including exhumed specimens from operational tailings disposal areas. These experimental analyses involve gradient ratio tests with varying values of stress levels and hydraulic gradients and based on different definitions of the gradient ratio (GR) aiming to pick up a more representative interface behaviour (GR_{25mm} by ASTM, 1996; GR_{8mm} by Fannin *et al*.,1994 and GR_{3mm} by Gardoni, 2000). The subscripted values refer to the predetermining distances from the GR equipment and indicated in Figure 3.18.

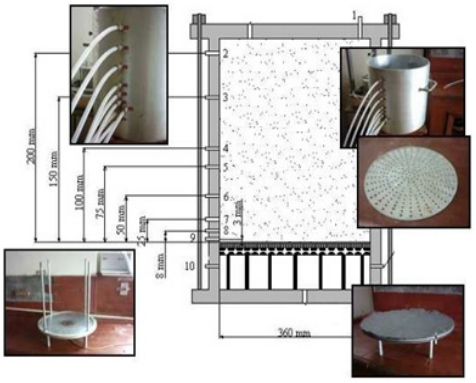

Figure 3.18. Gradient ratio equipment (Araújo *et al*., 2007).

Palmeira *et al*. (2009) present results of a series of GR tests performed on systems consisting of tailings from iron and phosphate mining plants and non-woven geotextiles (Figure 3.19). The filtration tests were performed under constant and varying system hydraulic gradients, and reached normal stresses up to 2000 kPa.

Figure 3.19 shows the variations of gradient ratios with total system gradient ($i_{system} = i_{1\text{-}10}$ in Figure 3.18) and with normal stress for tests on ore tailings from drying cells and nonwoven geotextile made of continuous fibrers of polyester with a mass per unit area of 400 g/m^2 and a variation range of filtration opening size between 0.09 and 0.16mm. Figure 3.19a shows a significant increase in GR values, particularly for GR_{3mm}, which would be caused by the migration of fines towards the geotextile filter. A continuous drop of gradient ratios can be observed in Figure 3.19b, particularly for normal stresses up to 500 kPa, due to the destruction of the arrays of particles formed at the tailings-geotextile interface caused by the increasing normal stresses.

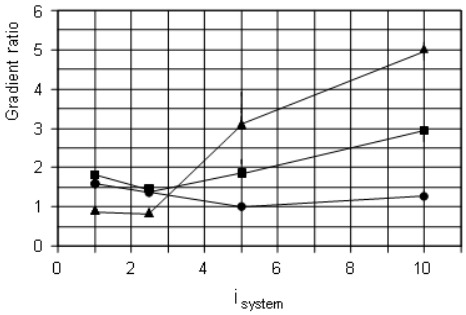

(a) GR versus system hydraulic gradients.

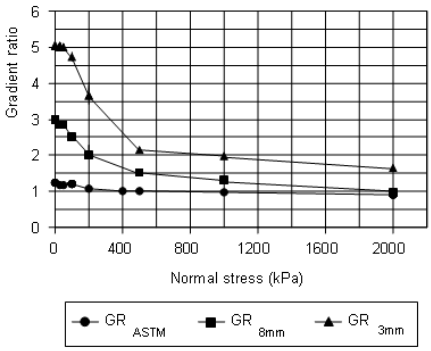

(b) GR versus normal stresses ($i_{system} = 10$).

Figure 3.19. Results of GR tests on tailings – nonwoven interfaces (Palmeira and Gardoni, 2009).

Araújo *et al*. (2007) analyzed the performance of nonwoven geotextile filters in contact with tailings based on GR and HCT tests. In the second case, the tailings-geotextile compatibility is evaluated using seepage induced consolidation tests. The results are commonly expressed in the form of void ratio-effective stress and void ratio-permeability relationships related to fine tailings in the presence or not of geotextile interfaces. Figure 3.20 presents HCT results for interfaces composed of an iron ore slime tailings collected in a driving cell, 250m from the discharge point, and different nonwoven geotextiles with mass per unit area of 150 g/m^2 (G1), 250 g/m^2 (G3) and 400 g/m^2 (G4), respectively.

These tests are very useful in investigating the compatibility between tailings and geotextile filters under different conditions of hydraulic gradients and confining stresses. In most situations, they become essential because of the severe operational conditions of these drainage systems in tailing dams, besides the local complex flow conditions, high stress levels and typical heterogeneity of tailings. More

yet, for the complex conditions found in these drainage systems of drying bays, the results obtained have evidenced the relevance of adopting an integrated methodology (incorporating results from a disposal simulation in flume apparatus, for example) to reproduce effective tailings deposition conditions.

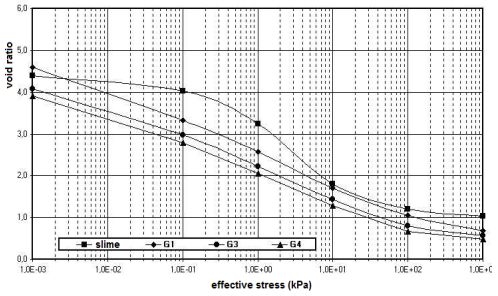

(a) compressibility tests

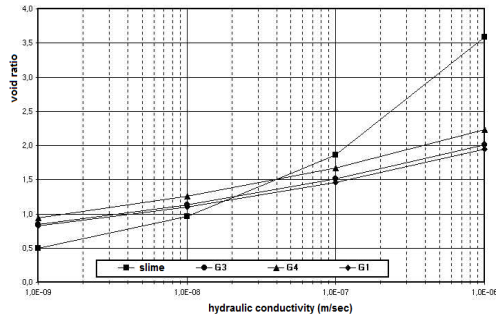

(b) hydraulic conductivity tests

Figure 3.20. Consolidation tests results in slime tailings – nonwoven geotextile interfaces (Araújo *et al*, 2007).

In fact, the application of such a methodology for exhumed specimens has demonstrated that the impregnation effects have been considerably higher than those observed in the laboratory tests. Besides the procedures of preparing tailings samples in the laboratory have limitations in reproducing the behaviour of the geotextile in the field for the actual conditions that occur in a tailings deposition process (Palmeira *et al*., 2009).

CASE 6: PHOSPHATE TAILINGS DEWATERING USING GEOTUBES (Gomes, 2007; Bittar, Gomes, Melo & Martins, 2010; Mazon, 2009)

In Brazil, carbonatitic phosphate exploitation is limited to a few mines that occur along the margins of the *Paraná* Sedimentary Basin in SE Brazil. In these mines, apatite ores have been extracted from the carbonatites and the typical P2O5 content of the deposits commonly reaches 30% or higher of apatite in secondary ore deposits and usually < 15% or up to 4% of apatite in primary ore deposits. In general, a deposit that predominantly contains primary apatite tends to show lower phosphate average grade and a less significant variation of the CaO/P2O5 ratio, typically ≤ 1.3 (Alves, 2008).

In the chemical plant, the apatite concentrate is converted to phosphoric acid via the sulfuric acid process route. Then, phosphoric acid is used to manufacture mainly fertilizers and animal feed. In the case of phosphate rock treatment processes, with lower P2O5 contents, three different types of tailings are always generated: tailings from a magnetic separation process, flotation tailings and fine tailings from comminution, classification and flotation processes (`slimes'). Initially the apatite ore undergoes removal of magnetite using wet magnetic drums, generating a residue rich in magnetite and ilmenite. After magnetic separation, a set of cyclones is used to deslime (i.e., remove the fines from the ore slip), and finally, the flotation is applied to separate apatite from the remaining minerals. The flotation tailings typically contain less than 1.5% of P2O5.

Diverse applications of these resulting tailings were subsequently developed, as they are economically useful for the cement industry (both carbonate and magnetite concentrates). The carbonate tailings with high magnesium are utilized as a soil additive. Part of the fragmented (blasted) residues is further crushed and sold as construction aggregate.

Phosphate slimes from chemical plant are constituted of very fine tailings (100% particles below #200) and have low solid content (normally below 10%), high plasticity (typical values are w_L = 80% and I_P = 40%) and reduced permeability (hydraulic conductivity coefficients in the order of 10^{-9} cm/s) and its disposal presents a great problem. These residues are discharged into large settling ponds (Figure 3.21) where the extremely fine suspended solids remain in the water for relatively long periods of time before settling to the bottom of the ponds or dams. The process is too slow and transforms large areas into unsightly and dangerous lagoons. This fact, in addition to the potential applications of these residues as industrial sub-products, has formed a favorable scenario to submit them to dewatering techniques.

In the dewatering method context, geotextiles permit a great variability of applications in the form of hydraulically filled tubes. This conception differs from other dewatering methods because the pulp material is surrounded and encapsulated by the filtration system. In some applications, the use of flocculating agents for improving or increasing the dewatering process of contaminated residues is required. In function of the specific nature and high water content of fine tailings, the filtration mechan-

isms of the geotubes, therefore, demand special approaches in the laboratory and field.

Figure 3.21. Phosphate tailings lagoon: general view

Representative samples of phosphate slimes from the *Cajati* Mine (90% particle sizes below 325 mesh), a mining complex located in the State of *Sao Paulo*, that is currently producing apatite from one of the world's lowest phosphate average grade deposits, were collected directly from the discharge point, homogenized with overlying site-water and placed in glass jars.

In laboratory tests, different polymers and other chemical conditioning agents were used for the effective separation of fine-grained solids from water (Figure 3.22a). These additives were evaluated based on the water release rate, water clarity, flocculent appearance, and water volume after passing through a geotextile filter. In addition, dosing rates were determined during these bench-top dewatering experiments and recommendations were provided as a part of these trials. In the field, geotube hanging bag and geotube model tests (Figure 3.22b) were performed based on the recommended previous chemical analyses to evaluate filtrate quality and time to attain desired cake solids within the geotube container.

The initial average solid percent in geotube model tests was 12.6%. The maximum percent solids increased to 69% and 74.7% after 48h and 10 days, respectively. The water content ranged from 31 to 25.3% in this monitoring period. The chemical composition of the dewatering tailings indicated, in its average composition, contents of 3.73% total P_2O_5, 49.6% CaO and 4.25% MgO. Additional information on the laboratory and field test results is reported by Bittar et al. (2010).

Although in the current design, the preliminary requirements are based on geotextile tubes that had a circumference of 36.5 m, a height of 1.5 m and lengths of 47m, 56m and 65m, for a stacked three-geotube configuration.

Figure 3.22. Dewatering geotube evaluation: chemical and geotube model tests (Bittar *et al*., 2010)

Alternative conceptions using geotubes have been proposed for the raising embankments design in upstream method tailings dams in Brazil. This is the most economic construction method for dam raises. The projects imply some kind of co-disposition process, involving granular tailings and fine tailings encapsulated in geotubes. This technique is particularly interesting in tailings disposal systems provided by hydro-cyclones (more efficient way to separate the larger tailings sand sized particles from the finer sized slurry sands, silts and clays by the use of centrifugal force) or in phosphate plants that generate residues composed of larger sand particles and finer slurry materials, separately.

The upstream method relies on the strength and drainage of the perimeter slimes deposited and settled tailings beach material for raised dyke construction. In addition, the coarser tailings beach materials are deposited around the perimeter of the impoundment to provide better strength, drainage and containment for the finer low strength tailings. An alternative model consists of incorporating geotubes with slimes as structural elements of the dam's upstream slope (Figure 3.23).

The most important factor in upstream method dam stability is an adequate tailings beach drainage, which requires the ability to deposit settled tailings above the impoundment water pool level. Therefore the lowest risk for the upstream method dams is to have the water pool located as far away from the

dam as possible after discharge operations. For improving dam stability, granular tailings deposit stacked up against the upstream slope dam have been an adopted solution. Another alternative will be to insert geotubes into the stacked deposit, in orderly arrangements involved by granular tailings, forming structures called 'geoberms' (Figure 3.24).

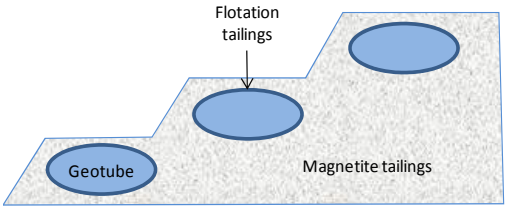

Figure 3.23. Geotubes as structural elements in upstream method phosphate tailings dams (Gomes, 2007).

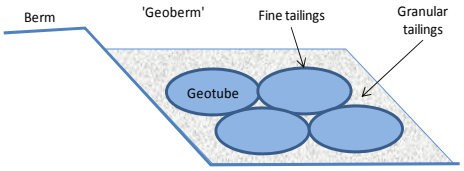

Figure 3.24. Geotubes as structural elements in 'geoberms' (Gomes, 2007).

Many mining impoundments have developed alternative and innovative methods of tailings management using large-scale geotextile tubes for the dewatering of tailings fines. However, in great mining facilities, the dewatering process through multiple geotubes can be inefficient and expensive, in function of the magnitude of the generated tailings volumes.

In such conditions, geotubes could be replaced by an open filtration structure, as a kind of a 'textile fence' for a more simple and cheaper dewatering process of the granular portion of flotation tailings or for magnetite phosphate (or other coarse-grained) tailings. As previously discussed (Case 5), the behaviour of geotextile filters in tailings disposal areas is very complex and requires a test methodology that more realistically simulates tailings deposition conditions. In principle, the main issues for the use of geosynthetic drainage systems in such structures are essentially similar to those already discussed in drying bay systems.

In these facilities, the tailings are deposed along a series of raised cells to promote the sequential consolidation and desiccation processes. These cells are partially confined by the 'textile fences', constructed with pre-fabricated elements or in-place geotextile panels that are raised concomitantly to cell disposition (Figure 3.25a). In Brazil, the technique has been applied in the *Quadrilátero Ferrífero* region (Mazon, 2009), for increasing the storage capacity of ore tailings disposal areas (Figure 3.25b).

(a)

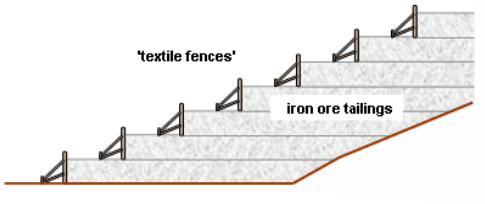

(b)

Figure 3.25. Tailings dewatering using 'textile fences" (Mazon,2009)

4 GEOSYNTHETICS IN LANDFILL

4.1 *Introduction*

The stringent environmental regulations, worldwide issued in the last years of the XX century, have called the attention for the correct disposition of all kinds of residues, especially solid waste. The option of dumps begun to be abandoned in favor of landfill, an engineered structure that comprises many elements, such as liner and cover systems with leachate and gases collection components. This item deals with some aspects of the use in Brazil of geosynthetics in landfill, showing examples of applications as well as some results of research.

4.2 *Brief note on recommendations and standards directed to environmental protection*

The concerns about adequate disposition of all kind of waste have long been recognized in Brazil. For instance, CETESB, the environmental agency of the State of São Paulo, has issued, in 1985, some recommendations about industrial waste that were re-

vised in 1990 (CETESB, 1993). Landfill was considered as an option for final disposition of residues, including hazardous and non-hazardous ones. As far as impermeable barriers are concerned, many of possible alternatives of cover and base were recommended. Figure 4.1 illustrates two of those options for non-hazardous and non inert waste. As can be seen the options take into account climatologic and hydro-geological site conditions in defining the need for barriers and explicitly states the option of using geomembranes as composing the barrier layers liner.

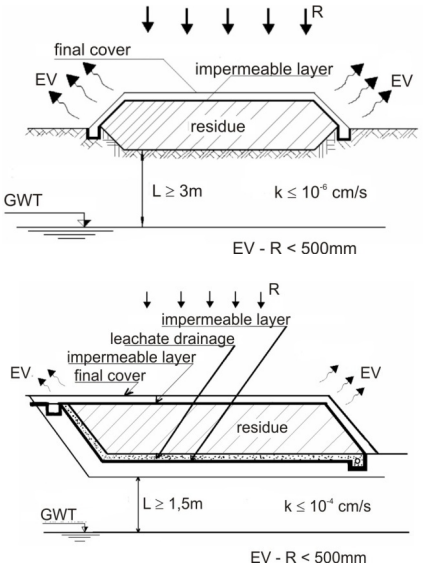

EV – Average annual Evaporation
R – Average annual Rainfall

Figure 4.1: Examples of recommendations for liner systems of non-hazardous, non inert waste, as a function of climatologic and hydro-geological site conditions (adapted from CETESB, 1991)

The subject of landfill is also addressed by many Brazilian Technical Standards that have incorporated some of the international practice related to landfilling, specially the topics associated to liner systems. The Standardized recommendations indicate for hazardous landfill the need of cover and/or base liners systems, with a component for leachate detection and collection under the bottom liner (ABNT – NBR 10157). There are no restrictions about the use of geosynthetics in all parts of liner and cover systems. Non – hazardous landfill, and in special municipal solid waste (MSW) landfill, depending on site conditions, needs at least an impermeable barrier, which can be built with geomembranes (ABNT – NBR13896). Federal, state and municipal legislation is available in Brazil to deal with environmental questions. The landmark of this legislation is the National Environmental Policy and the creation of the National Environmental Council (CONAMA), in 1981, that edited many resolutions, including the 01/86 that disciplined the criteria for environmental impact analysis. Subsequent legislation has tighten the rules for engineering design and construction and led to complex licensing procedures during which the many measures that must be fulfilled to protect the environment are settled.

4.3 *Case history*

Probably, one of the first uses of geomembranes in Municipal Solid Waste (MSW) landfill occurred around 1990 at São João landfill, in the city of São Paulo, which received about 7500 ton of municipal solid waste per day. In this case, a single PVC geomembrane, 2mm thick was used, above a compacted clay liner. Later on, the practice of using geomembranes and other geosynthetics has spread to landfills that serve medium to large cities and soon the geomembrane of choice begun to be HDPE, even though in many places the option continued to be PVC. Although the scenery around the country is not optimistic regarding MSW landfill, as much uncontrolled dumping continues to be common practice in many places, it is worth to recognize that sounder environmentally solutions are available and much of those solutions were improved by the use of geosynthetics. In MSW landfill, solutions depart from the simpler option of geomembrane over compacted clayey soil and reach more elaborated sections, with intensive use of geosynthetics. For instance, Figure 4.2(a) shows the liner section designed for non-hazardous landfill, the CTR Caieiras, composed by compacted clayey soil, a 2 mm thick HDPE textured geomembrane, a drainage geocomposite (HDPE geonet coated with non-woven geotextiles with mass by unit area of 400 g/m^2) for leachate drainage. Mechanical protection is provided by selected waste with coefficient of hydraulic conductivity lower than 10^{-3} cm/s (Vidal, 2003). Figure 4.2(b) shows a detail of geosynthetics deployment at the CTR Caieiras, where one can appreciate the geomembrane and the drainage geocomposite.

Figure 4.3 illustrates some typical liner and cover sections for hazardous landfill. Discarding some minor variations, Fig. 4.3(a) shows what can be considered a typical bottom liner composed of double geomembranes. A coarse granular layer associated with a geopipe, above the primary geomembrane, serves as drainage for the leachate. Between the primary and secondary geomembranes, there is a leak detection layer composed also by a coarse granular layer and geopipe. This double liner usually rests over properly low-permeability compacted soil.

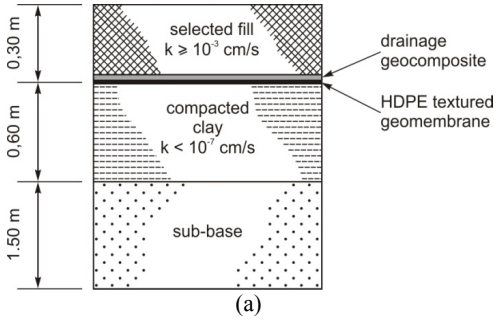

(a)

(b)

Figure 4.2: Example of liner used in MSW landfill in Brazil. (a) cross section; (b) HDPE geomembrane and drainage geocomposite deployment (Vidal, 2003).

The use of geosynthetics is more intensive in side slopes where the granular layers are usually substituted for a drainage geocomposite above the primary geomembrane liner and a geonet between geomembranes to act as a detecting layer. In some instances, GCL has been used instead of compacted soil or to compose a geocomposite double liner.

Figure 4.3(b) shows a cover section of a deposit of waste from cast iron industry. In this case, there is a gas drainage layer and a gas collecting pipe; non-woven geotextile for separation and protection; a GCL forming an impermeable layer and a drainage geocomposite to collect infiltrating water.

Geosynthetics are also extensively used in the rehabilitation of old dumps and residues deposits. Costa Filho et al. (2002) and Costa Filho & Sieira (2008) report the rehabilitation of an old residue deposit from an aluminum plant.

The residue is very soft saturated clayey silt with pH between 12 and 13 and some heavy metals. The deposit reaches about 16m depth and occupies an area of about 25ha. The solution adopted comprises a composite cover, with many components, such as an impermeable layer and a drainage layer to collect the liquor from residue consolidation. The final arrangement of rehabilitated area is shown in Figure 4.4 , while two cross sections and some details of the cover configuration are shown in Figure 4.5.The following elements compose the complete cover system:

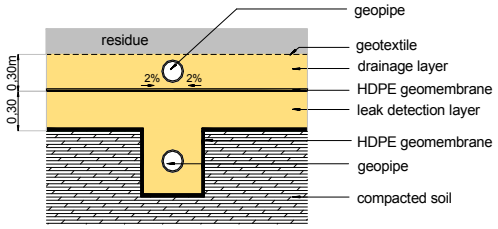

(a)

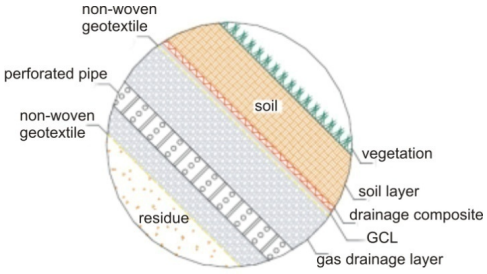

(b)

Figure 4.3: Examples of liners used in hazardous landfill in Brazil. (a) bottom liner (adapted from Nahas, 2009); (b) final cover system (adapted from Maccaferri, 2007)

• a drainage layer on the residue surface to collect and direct to the industrial plant the liquor ascending from the residue due to the load to be placed. This layer is formed by alternating strips of drainage geocomposite (polyethylene geonet, between 2 heat bonded polypropylene geotextiles) and non-woven geotextile (needle punched, polypropylene, mass per unit width 400 gr/m^2). Figure 4.6 illustrates the drainage layer configuration, which was adopted to reduce costs, since the initial option was for using only drainage geocomposites.

The configuration combines strips of drainage geocomposites 4m width and non-woven geotextiles, 8m width, which are standard factory dimensions. To improve drainage performance, 8 drainage trenches were excavated in the residue in the upstream-downstream direction. Figure 4.7 illustrates the drainage trench, with flexible, slotted geopipes of polyethylene.

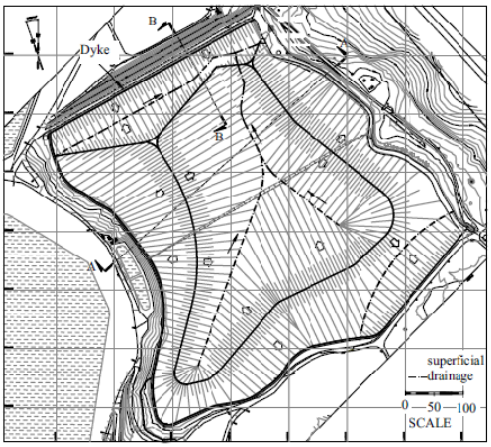

Figure 4.4: Final arrangement of rehabilitated area (Costa Filho et al., 2002)

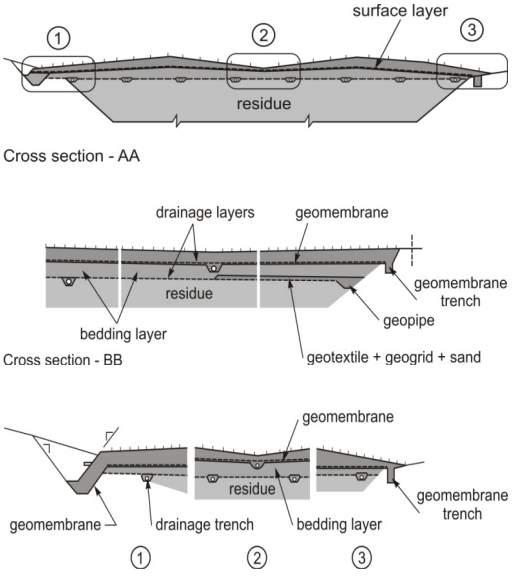

Figure 4.5: Cross sections and details of waste deposit rehabilitation configuration. (adapted from Costa Filho et al., 2002)

• as softer residue was found along the valley closure dikes, difficult construction conditions were previewed. To overcome those difficulties, a sand layer wrapped by woven geotextile (polypropylene, tensile strength of 55kN/m and 35kN/m, in the longitudinal and transversal directions, respectively) was used in order to provide adequate drainage and support for machinery. However, in some parts, a geogrid (biaxial geogrid PVA, tensile strength of 70kN/m) was used as reinforcement under the drainage layer.

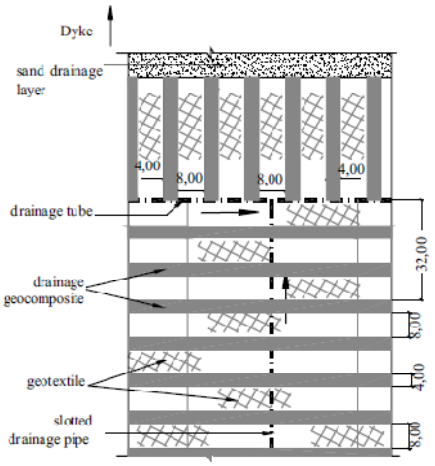

Figure 4.6 – Arrangement of geosynthetics to drain liquor ascending from the residue (Costa Filho et al., 2002)

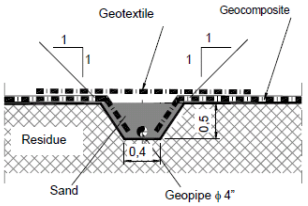

Figure 4.7: Cross section of drainage trench

• to deal with the settlement of the residue and maintain the surface grade, a variable height compensating (bedding) fill layer was constructed.

• an impermeable layer composed of compacted soil and a flexible geomembrane (PVC, 0.8mm thickness) was constructed over the compensating layer of soil;

• a drainage layer to collect the infiltrating water. This was similar to the drainage layer of residue. As there were many concerns related to the drainage capacity and considering the settlement of the residue, that in some cases could reach about 1500mm, it was decided to install flexible slotted geopipes in ditches apart about 25m and disposed obliquely to the drainage strips.

• Capping the cover system, a final conformation organic soil layer was spread to support the vegetation.

All the rehabilitation works took place between 2000 and 2001 and its performance was very good as indicated by the monitoring of settlement and drainage of residue. The use of geosynthetics could improve design and construction of landfill, since the very tight construction schedule could only be met with the use of prefabricated materials. For in-

stance, the geomembrane panels were factory seamed thus allowing deployment with little field seams and the drainage panels deployed with factory widths. About 260,000 m3 of liquor was collected by 2007 and the most part was associated to the consolidation of the residue (Costa Filho and Sieira, 2008). The performance of the drainage layer was very good. In spite of the fact that the residue is in direct contact with the geotextile, clogging was not noticed.

Another example is the rehabilitation of the entire area where a landfill of hazardous waste from a chemical plant is inserted. The design also considered the many problems occurring such as slope instability as well as tried to recompose the topographic features of the area that reached 215.000 m^2

Figure 4.8 (a) sketches the configuration of the area and the occurrence of groundwater that was reached by the contaminating plume, while Figure 4.8(b) sketches the final configuration of the area with the rehabilitation measures that were taken.

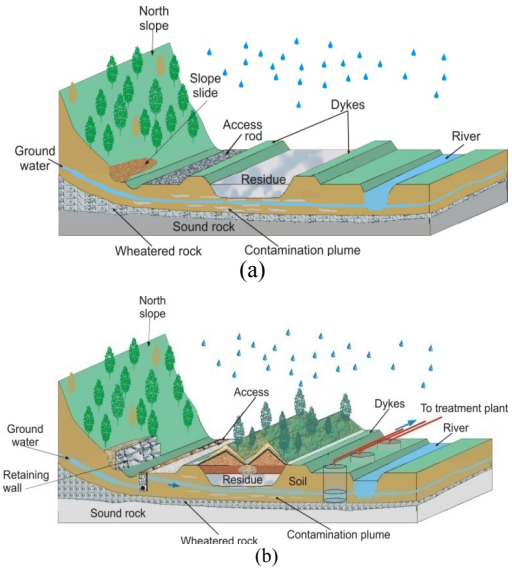

Figure 4.8: Artist's rendering of degraded area showing the hazardous waste deposit.(a) before; (b) after rehabilitation works (Oliveira, 2009).

The solution adopted considered a hydraulic barrier disposed upstream to reduce ground water flow below the residue. Another hydraulic barrier was constructed downstream to pump the contaminated water that was conducted to a decontamination plant. The hazardous waste deposit was covered with soil to avoid infiltration and to recompose the original topography. Figure 4.9 shows the components used in this rehabilitation that included a woven geotextile for reinforcement and to support the earthfill. A PVC geomembrane was placed above the earthfill as an impermeable layer and a non-woven geotextile to drain the rain infiltration. A protecting layer of soil was placed above those components, which served also to support the vegetation.

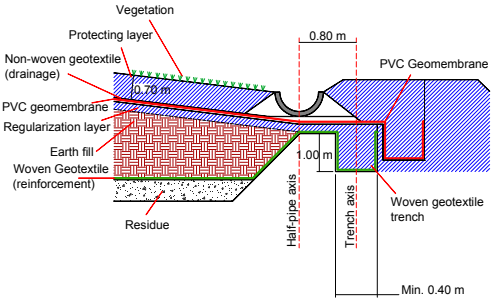

Figure 4.9: General configuration of components of hazardous waste deposit rehabilitation. (Oliveira, 2009).

In some parts of the deposit that were difficult to access, a geotube was used to ease the earth filling works and to serve as a firm base for some parts of the superficial drainage system, as illustrated in Figure 4.10. The geotube was built with geotextile filled with sand. The slope slide was stabilized with the aid of drainage and retaining walls. In addition, superficial drainage was disposed on the total area, which was also revegetated. The earth work reached 480.000 m^3 of soil excavation, transport and compaction.

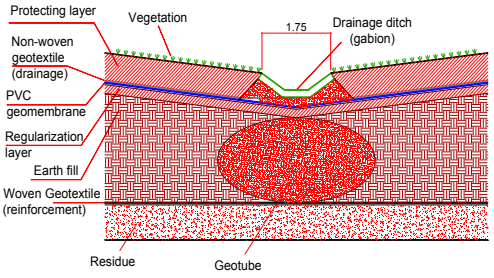

Figure 4.10: Components of hazardous waste deposit rehabilitation, including geotube. (Oliveira, 2009).

4.4 *Brazilian research about geosynthetics in landfill*

Research about the behavior and performance of geosynthetics used in landfills has been centered in some Universities, mainly in the University of Brasilia (UNB) and in the University of São Paulo at São Carlos (USP). Many topics have been addressed

such as the clogging of geotextiles, mechanical protection of geomembrane, ageing and degradation of geosynthetics and interface shear strength between geosynthetics and geosynthetics and soil. Due to space limitations, only a synthesis of some of those investigations will be presented and the reader is referred to the original papers for further details.

Regarding the clogging of geosynthetics during leachate flow, Silva et al. (2002) have conducted column tests using granular and synthetic filters, non-woven, needle punched polyester geotextile of different mass per unit area and filtration characteristics. Raw leachate was continuously percolated and a 95% reduction of flow rates was observed after 4h of testing. This result was associated to the severe conditions of flow, considered not representative of field conditions (Palmeira, 2006). The main mechanism of flow reduction was geotextile blinding caused by the large amount of solids in suspension. Reverse flow under a hydraulic head of 18cm was able to disrupt the blinding layer until next blinding.

To consider a more representative field characteristics of leachate, Colmanetti and Palmeira (2002) have built experimental waste cells using tanks with 580mm diameter and 815 mm height, with different drainage systems: gravel layer; gravel layer associated with different geotextile filters (GA and GB) and sand and gravel layers. Table 4.1 gathers the geotextile characteristics and properties.

Table 4.1. Characteristics of the geotextiles used in the tests (Colmanetti and Palmeira, 2002).

Property	GA	GB
Mass per unit area (g/m^2)	600	300
Thickness at 2 kPa normal stress (mm)	4.5	2.6
Porosity (%)	90	92
Normal permeability (cm/s)	0.24	0.4
Permittivity (s^{-1})	0.9	1.5
In-plane permeability (cm/s)	0.6	0.6
Transmissivity (cm^2/s)	0.27	0.13
Filtration opening size – FOS (mm)	0.06	0.11
Aparent opening size – AOS (mm)	< 0.11	0.12-0.17

Notes: FOS and AOS values obtained according to CFGG (1986) and ASTM (1995), respectively.

At the beginning of tests, only the naturally generated leachate was allowed to percolate and, after the 68th day of testing, water was added at a rate of 5 liters/week. Much data was obtained during the tests, such as the temperature of the waste and the chemical composition of the effluent, the micro organisms growth and the effluent volume with time. At the end, the tests were dismantled and additional tests were performed such as geotextile permittivity.

The effluent rate, normalised by the waste mass, was smaller for geotextile GA and for the sand and gravel filter arrangement. In accordance with the effluent rate measured, they retained the largest percentages of total solids. Samples of geotextile were taken and tested for hydraulic conductivity, which was reduced about 80% in geotextiles GA and GB. The hydraulic gradient was increased during the test to verify if entrapped particles could be washed out thus increasing the permeability; however, the increase in permeability in most of the tests was small. Figure 4.11 shows the comparisons between the permeabilities of virgin and exhumed geotextile specimens.

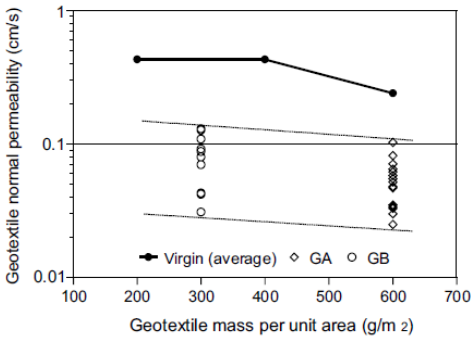

Figure 4.11. Comparison between permeability coefficients of exhumed and virgin geotextile specimens (Colmanetti and Palmeira, 2002)

Junqueira et al. (2006) have constructed large experimental test cells with different drainage systems above a HDPE geomembrane: a 0.2m thick sand blanket and a draining geocomposite (polyethylene geonet and non woven geotextile cover (mass per unit area = 1800 g/m^2; thickness = 7.7mm; permittivity = 1.6 s^{-1}; transmissivity = 0.11 cm^2/s and filtration opening size of non woven geotextile = 0.114 mm). Figure 4.12 illustrates experimental cells configurations.

The data measured included precipitation and effluent volumes over time. They revealed the time lag characteristics of the two draining systems: while in the geocomposite precipitation and effluent volumes were almost simultaneous, no flow occurred in the sand blanket until the field storage capacity of the sand layer was fulfilled, what took about 20 months of test.

Exhumation after 5 years has shown that both systems were contaminated by solid particles and the growth of biofilms, which were more pronounced in the sand layer, reaching a few millimeters thickness. In the geotextile of the drainage geocomposite, low levels of impregnation by solid particles were observed as well as low amount of biofilms thus indicating a superior behavior of geotextile. Although the performance of the sand filter was satisfactory

after 5 years of service, the observations suggest that the sand may clog during its lifetime.

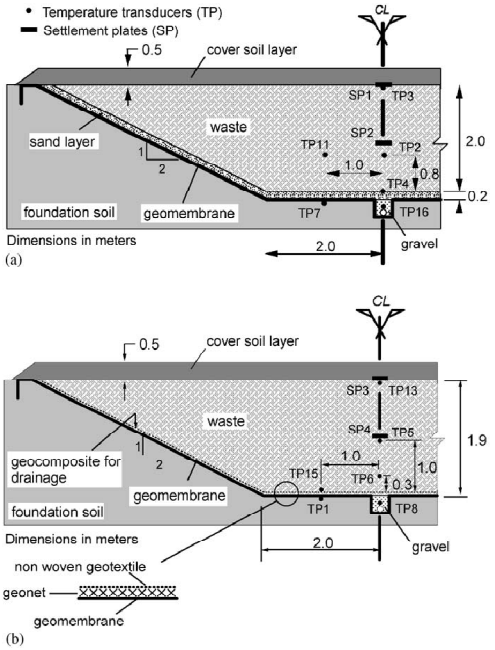

Figure 4.12: Experimental waste cells to investigate the clogging of different draining systems (a) sand drainage system—cell CS and (b) geocomposite drainage system—cell CG (Junqueira et al., 2006).

Palmeira et al. (2008) have performed permittivity tests on three types of non-woven, needle-punched, geotextiles made of continuous polyester fibers. The mass per unit area of GTA, GTB and GTC specimens were 100, 300 and 600 g/m2, respectively, and filtration opening sizes varied between 0.06 and 0.15mm. Microscopic investigations, chemical and bacteriological tests as well as back flush tests after filter clogging were performed. The leachate was first filtered to remove solids in suspension and the test results have shown a great reduction in hydraulic conductivity caused by biological clogging already in the first day of test, when hydraulic conductivity was reduced by values between one and two orders of magnitude and continued until the end of tests, following different trends. The inspection of the geotextiles has shown that the clogging mechanism was concentrated in the first layers of fibers of the geotextile. It was also observed that the reduction of hydraulic conductivity could be related to the increase in biomass within the geotextile; however, for the materials and tests conditions used, the biological clogging could not be related to materials properties, such as thickness and fibers distribution. Tests have shown that similar hydraulic heads could wash the biofilm out for the three geotextile and suggest that in the case of filter clogging, continuous leachate mounding can lead to filter's breakthrough. Additional analysis was performed considering bacteria growth and hydraulic modeling of biofilm clogging and the authors concluded: "*Biological clogging of geotextiles subjected to the flow of leachate is a very complex phenomenon and much research is still required for a better understanding and prediction of such process*".

The degradation of geosynthetics and in special of geomembranes has been a topic of concern among many Brazilian researchers (Maia & Vilar; 2002; Matheus et al., 2004; Silva et al., 2007; Lodi, 2003; Lodi et al., 2008(a) and(b)). To some extent, the results of the researchers coincided considering the ageing effect of common agents, as UV, temperature and exposition to different kind of leachate. For instance, Lodi (2003) has studied the degradation of HDPE and PVC geomembranes after being exposed to different ageing effects, such as UV and water condensation, domestic sewage, temperature and the compatibility with Niobium residue. Different times of exposure were used and various mechanical and chemical tests, such as Thermo-Gravimetric Analysis (TGA), Melting Flow Index (MFI) and Oxidation Induction Time (OIT), were performed to compare virgin and degraded properties. A common feature of mechanical index tests was the erratic variation of properties over time, with variation within the suggested limits reported in the literature. This is considered as an indication of non-degradation of the GM (Koerner, 1998). However, Lodi et al (2008) has suggested the use of MFI test to help interpreting the mechanical tests after incubation of HDPE geomembrane. In their tests it was possible to measure different MFI values between virgin and incubated geomembranes and thus inferring that the degradation has already begun in many of the incubated geomembranes.

Many researchers such as Nascimento and Palmeira (2002); Rebelo (2008) and Geroto (2008) have addressed the protection of geomembranes. Rebelo (2008) and Geroto (2008) have tested many options of geomembrane protection in laboratory and field tests. Geomembranes used were of PVC, 1.0 and 2.0 mm thickness, and HDPE, 1.5 and 2.0 mm thickness. Protection layers were of non-woven polyester and polypropylene geotextiles, with mass per unit area ranging from 150 to 600 g/m^2, a medium to fine sand and a clayey sand typical of the State of São Paulo. The main characteristics of the geosynthetics used are in Tables 4.2 and 4.3.

Lab tests included static and dynamic puncture tests and cycling load and revealed some correspondence between geotextile properties and improved resistance of the geomembrane – protection system. The test results have shown that the improvement of resistance was related to the mass per unit area of

the geotextile, but depended on the type of the geotextile. In the search for a common relationship, the test results were considered as dependent on the tensile resistance of geotextiles. Figure 4.13 shows the puncture resistance increment (ΔFp) of geomembrane – geotextile system against the tensile stress of geotextile (σ_{GT}).

From Fig. 4.13(a) it can be seen that the increase in geomembrane protection is directly related to the geotextile tensile resistance and that the beneficial effects of the protection layer is more pronounced in the less resistant geomembrane, PVC in this case. A common trend for all the geomembranes and geotextiles used in the tests can be seen when the increment in resistance is plotted against the ratio between the tensile resistance of geomembrane and tensile stress of geotextile as shown in Figure 4.13(b). In this figure, it can be seen the superior performance of the double protection, that is, the geomembrane sandwiched between two geotextiles and the almost similar behavior of the combinations of geotextile under or above the geomembrane.

Geroto (2008) has performed additional investigation about the behavior of protection elements, by conducting index, static loading and hydraulic punching tests (ASTM D5514). The latter, besides standardized conditions, was also performed considering some adaptation in order to include different gravel shapes. This testing variation allowed distinguishing between different failure modes: HDPE geomembrane was more susceptible to punching rupture, commanded by the pointy stones; while the more flexible geomembrane, PVC, tends to involve the stone and fail by a process similar to tearing

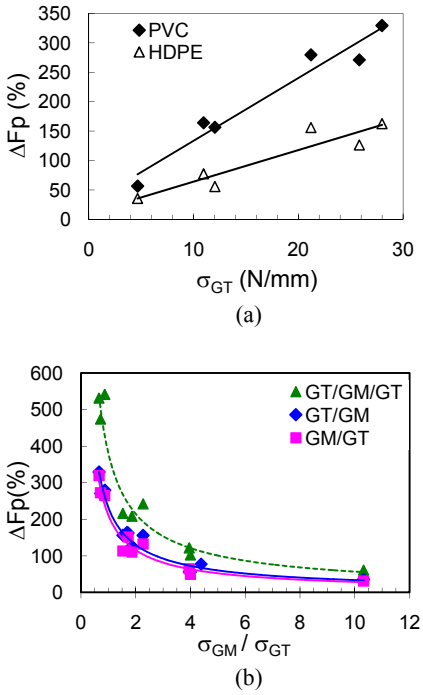

Figure 4.13. Puncture test results of the geomembrane and protection geotextile system.

Table 4.2: Main characteristics of the geomembranes used to investigate geomembrane protection (Rebelo, 2008; Geroto, 2008)

Test	Standard	Units	Geomembrane			
			HDPE 1.5	HDPE 2.0	PVC 1.0	PVC 2.0
Water vapor transmission	ASTM E 96	g/Pa.s.m	$2.8.10^{-13}$	$1.8.10^{-13}$	$1.2.10^{-12}$	$1.1.10^{-12}$
Puncture Resistance	ASTM D 4833	N	710	744	315	560
Tensile:(1) Index	ASTMD 6693(2)/ D 882(3)	N/mm	33	36	17	30
		%	16	16	394	474
Tensile: wide width(1)	ASTM D4885	MPa	21.1	15.3	11.9	10.7
		%	18	36	293	275
Tensile -Axi – Symetric(1)	ASTM D5617	MPa	25.6	-	10	-
		%	62	-	100	-

(1) yielding for HDPE, rupture for PVC; (2) for HDPE; (3) for PVC

Table 4.3: Main characteristics of the geotextiles used to investigate geomembrane protection.(Rebelo, 2008; Geroto, 2008)

Test		Standard	Units	Non – woven Geotextile				
				PET 150	PET 300	PET 400	PET 600	PP 600
Mass per unit area		ABNT 12568	g/m²	168.3	293.2	353.2	576.4	593.2
Thickness		ABNT 12569	mm	1.58	2.50	2.19	3.36	4.62
Puncture Resistance		ABNT 13359	kN	0.98	1.82	2.67	3.79	5.06
Tensile – wide width	Long.	ABNT 12824	N/mm	7.0	9.9	10.9	22.0	21.9
			%	69.0	93.5	73.6	77.7	82.2
	Transv.		N/mm	6.8	13.2	21.6	26.7	37.2
			%	98.5	92.6	55.4	75.6	62.3

Figure 4.14 shows the different pattern of rupture for HDPE and PVC geomembranes.

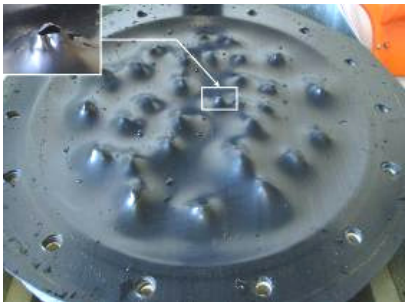

(a)

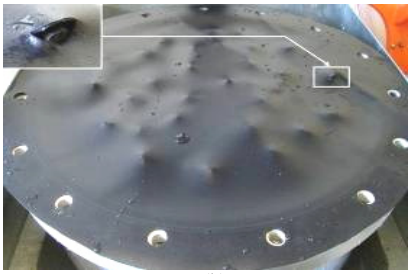

(b)

Figure 4.14: Different rupture features of geomembranes in the hydraulic punching test. (a) HDPE geomembrane; (b) PVC geomembrane.

The performance of the protection depended on the flexibility of the geotextile and on the different modes of failure observed. Less flexible geotextile, such as PET 400 and PET 600 tended to fail in a way similar to that observed for the HDPE, while the more flexible ones followed a rupture pattern compared to the observed for the PVC. The dominant rupture pattern of HDPE was by puncture and this probably resulted in a more homogeneous behavior of protection. The improvement in resistance was analyzed considering some index properties such as mass by unit area, thickness, punching resistance and tensile resistance, both in transversal and in longitudinal directions. It was observed that the variable that better represented the increase in resistance was the tensile resistance in the transversal direction of geotextile as shown in Figure 4.15.

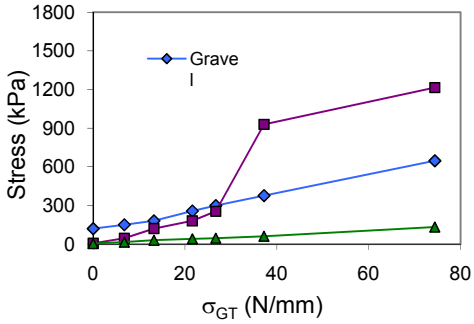

Figure 4.15: Hydraulic punching tests of protected HDPE against tensile resistance of protection geotextile.

Field tests designed to study mechanical protection of geomembrane comprised the construction of an experimental liner where various protection configurations were used and the typical constructive operations were simulated. Figure 4.16 shows some aspects of experimental liner construction. After the completion of operations, geomembranes were exhumed, visually observed, subjected to Spark test in the field and categorized according to the damage suffered. Selected specimens were then tested in laboratory in large width tension, axi – symmetric tension and stress cracking tests.

Visual observation showed that the best performance was associated to the soil and sand covers and to the geotextile with the largest mass per unit area. As expected, the unprotected geomembranes were the most damaged and showed large decrease in tensile and stress cracking resistance, as compared

to the virgin geomembrane. The different geotextile protection in the field, however, could not be associated with the tension resistance of geotextile (Figures 4.17 and 4.18) as was the case of the puncture tests.

Figure 4.16: Experimental liner construction and example of damage (hole) in exhumed geomembrane (Rebelo, 2008).

Another point was the different damages experienced by the geomembranes in the field that were larger than what was observed in the lab during cycling loading tests. The occurrence of tangential stresses during machinery operations probably was the responsible for these differences and should be considered in the improvement of laboratory tests that intend to study installation damages in geomembranes.

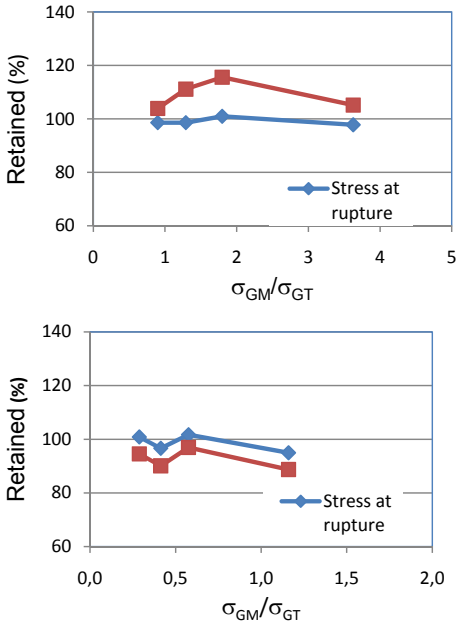

Figure 4.17: Retained stress and strain (large width tests) against the ratio between tensile stress of geotextile and tensile stress of geomembrane. (a) HDPE 1.5 mm; (b) PVC 1.0 mm

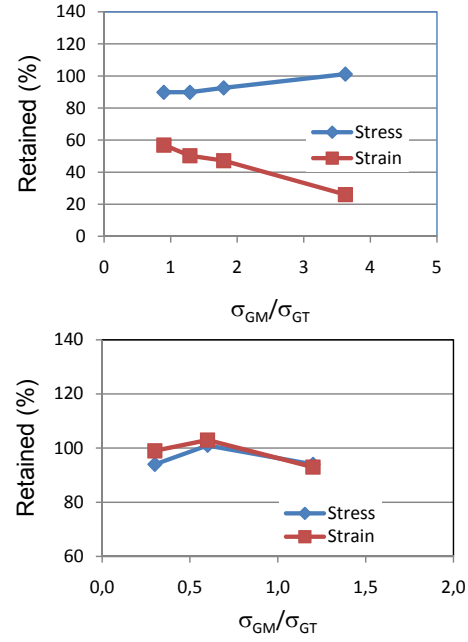

Figure 4.18:Retained stress and strain in axi - symmetric tension tests against the ratio tensile stress of geotextile and tensile stress of geomembrane. (a) HDPE 1.5 mm; (b) PVC 1.0 mm

5 CONCLUDING REMARKS

This paper has illustrated the use of geosynthetics in many kinds of engineering applications in Brazil. The few examples presented are only a sample of the many projects already finished and under way nowadays and attest that geosynthetics offer alternatives to design, are easy to install and perform in very convenient ways being almost a mandatory component in modern design and construction of landfills and in rehabilitation works. The excerpt of the research performed shows the capabilities of Universities interested on the subject of geosynthetics, which have already produced a wealth of results.

ACKNOWLEDGEMENTS

The first two authors would like to thank Clara N. Takaki, from Vecttor, Celso Correa, from Andrade Gutierrez, Henrique Magnani de Oliveira, from UFSC, A. Spotti from COPPE, Andre Silva and Dimiter Alexiev from Huesker (for information on case 2 of part 2) and to people at Geoprojetos (for help in formatting the paper). The third author would like to thanks Vale, Samarco, Bunge, Votorantin and DER/MG for allowing mention to jobs and to CAPES, CNPq and FAPEMIG for research financing and scholarships and to Leandro Moura Costa Filho. The fourth Author acknowledges the information provided by Leandro Moura Costa Filho, Ennio Marques Palmeira, Francisco J.P. de Oliveira and Claudio Nahas.

REFERENCES

ABINT (2004), "Brazilian Geosynthetic Manual" (in Portuguese: "Manual Brasileiro de Geossintéticos"), Coord. José Carlos Vertematti, Edgar Blücher, São Paulo.

ABNT - NBR 10157 (1987). "Hazardous landfill: Criteria for Design, Construction and Operation. Brazilian Association of Technical Standards, Rio de Janeiro. (in Portuguese) Standards, Rio de Janeiro. (in Portuguese)

ABNT - NBR 12568 (2003). Geosynthetics- Standard test method for measuring the mass per unit area. Brazilian Association of Technical Standards, Rio de Janeiro. (in Portuguese)

ABNT - NBR 12569 (1992). Geotextiles: Standard test method for measuring the thickness. Brazilian Association of Technical Standards, Rio de Janeiro. (in Portuguese)

ABNT - NBR 12824 (1993). Geotextiles: Standard Test Method for Determining the Wide Strip Tensile Resistance. Brazilian Association of Technical Standards, Rio de Janeiro. (in Portuguese)

ABNT - NBR 13359 (1995). Geotextiles: Standard test method for Index Puncture Resistance. Brazilian Association of Technical Standards, Rio de Janeiro. (in Portuguese)

ABNT - NBR 13896 (1997). Non hazardous landfill: Criteria for Designing, Construction and Operation. Brazilian Association of Technical Standards, Rio de Janeiro. (in Portuguese)

Abramento, M., Castro, G.R. & Campos, S.J.A.M. (2002), "Short and long-term analysis of a reinforced embankment over soft soil", 7th International Conference on Geosynthetics, Nice, France.

Alexiew, D., Brokemper, D & Lothspeich, S. (2005), "Geotextile encased columns (GEC): load capacity, geotextile selection and pre-designed graphs", *Proceedings of GeoFrontiers 2005*. ASCE, United States.

Almeida, M.S.S, Marques, M.E.S., Almeida, M.C.F. & Mendonça, M.B. (2008), "Performance of two "low" piled embankments with geogrids at Rio de Janeiro", First Panamerican Geosynthetics Conference, Cancún

Almeida, M.S.S, Spotti, A.F., Marques, M.E.S., Almeida, M.C.F. & Mendonça, M.B. (2007), "Structured fill with geogrid platform: Design and Behavior" (in Portuguese), Fifth Brazilian Geosynthetic Symposium, Recife

Alves, P. R. (2008). The Carbonatite-Hosted Apatite Deposit of Jacupiranga, SE Brazil: Styles of Mineralization, Ore Characterization, and Association with Mineral Processing. Master's Thesis, Geology & Geophysics, Missouri University of Science and Technology. 140p.

Araújo, G.S.; Gomes, R.C.; Almeida, M.G.G. (2007) Experimental Evaluation of the Filter-Drainage Behavior of Interfaces Composed by Fine Mining Tailings and Geotextiles. Proc. 5th Simp. Brasileiro de Geossintéticos/REGEO, Recife: ABMS / IGS-BR, CD (in Portuguese).

ASTM (1996). Standard test method for measuring the soil-geotextile clogging potential by the gradient ratio (D5101-96). Annual Book of ASTM Standards, Vol. 04.09, ASTM, Philadelphia, USA.

ASTM 1995. *ASTM standards on geosynthetics*. American Society for Testing and Materials, ASTM Committee D-35, Philadelphia, PA, USA, 178 p.

ASTM D 4833 (2007). "Standard Test Method for Index Puncture Resistance of Geomembranes and Related Products"

ASTM D 6693 (2004). "Standard Test Method for Determining Tensile Properties of Nonreinforced Polyethylene and Nonreinforced Flexible Polypropylene Geomembranes".

ASTM D4885 Standard Test Method for Determining Performance Strength of Geomembranes by the Wide Strip Tensile Method.

ASTM D5514 (1994). "Standard Test Method for Large Scale Hydrostatic Puncture Testing of Geosynthetics".

ASTM E 96 (2005). "Standard Test Methods for Water Vapor Transmission of Materials".

ASTM. D5617 (1999). Standard Test Method for Multi-Axial Tension Test for Geosynthetics.

ASTM. D882 (1995a). Standard Test Method for Tensile Properties of Thin Plastic Sheeting.

Aubeny, C.P., Li, Y. & Briaud, J.L. (2002), "Geosynthetic reinforced pile supported embankments: numerical simulation and design needs", 7th International Conference on Geosynthetics, Nice, France.

Becker, L. B. (2005) – Behaviour of Geogrids in a Reinforced Soil Wall and in Pull-out Tests – Ph.D. Thesis, Civil Eng. Dept, Catholic Univ., Rio de Janeiro (in Portuguese).

Bittar, R.J.; Gomes, R.C.; Melo, L.C.Q.C.; Martins, P.M. (2010). Phosphate Fine Tailings Disposal Systems Using Geotubes. In: 9th International Conference on Geosynthetics, Guarujá, Brazil (submitted paper).

BS8006 (1995), "Code of practice for strengthened/reinforced soils and other fills", British Standard

CETESB (1993) Industrial Solid Waste. Cia. Tecnologia Saneamento Ambiental, São Paulo, 233p. (in Portuguese).

CFGG 1986. *Normes Françaises D'Essais*. Comité Français des Géotextles et Géomembranes.

Colmanetti J.P. ; Palmeira, E. M. (2002). A Study on Geotextile-Leachate Interaction by Large Laboratory Tests. In: 7th International Conference on Geosynthetics, Nice. Proceedings. Lisse: Balkema, v. 2. p. 749-752.

Costa Filho, L. M.; Pedrosa, S. B. M.; Sieira, A. C. C. F.; Silva, M. R. P. (2006) Behaviour of an Upstream Stack Formed with Geotextile Wrapped Dikes. In: 8th International Conference on Geosynthetics, IGS, Yokohama.

Costa Filho, L.M. & Sieira, A.C.C.F.(2008).Recent Applications of Geosynthetics in Mining and Industrial Waste Disposal. Proc. *The First Pan American Geosynthetics Conference & Exhibition,* 2-5 March 2008, Cancun, Mexico.

Costa Filho, L.M.; Pacheco, E.B.; Paes, G.; Chianello, M. (2002) Extensive Use of Geosynthetics in the Rehabilitation of an Old Industrial Waste Deposit – In: Proceedings7th, International Conference on Geosynthetics, IGS, Nice, Vol.2, p 705 – 708.

de Mello, L.G., Mondolfo, M., Barbosa, G., Bilfinger, W. & Tsukahara, C.N. (2008b) "Successful use of geosynthetic for retaining structures and embankment construction", 1st Panamerican Geosynthetic Conference, Cancun, Mexico.

de Mello, L.G., Mondolfo, M., Gomes, J.C.M. & Caran, A. (2002), "Optimized design and construction of an urban highway embankment on soft soil", 7th International Conference on Geosynthetics, Nice, France.

de Mello, L.G., Mondolfo, M., Montez, F., Tsukahara, C.N. & Bilfinger, W. (2008a) "Extension of Vidoca Avenue: Successful use of geosynthetic for retaining structures and embankment construction", 1st Panamerican Geosynthetic Conference, Cancun, Mexico.

Fannin, R.J., Vaid, Y.P., Shi, Y., 1994. A critical evaluation of the gradient ratio test. Geotechnical Testing Journal 17, (1), 35-42.

Fernandes, G. (2005). Behaviour of geosynthetic reinforced railway tracks constructed with fine grained soils and mining wastes. PhD Thesis, Graduate Program of Geotechnics, University of Brasilia, Brasilia, Brazil, 253 p. (in Portuguese).

Fernandes, G.; Palmeira, E.M.; Gomes, R.C (2008). Performance of Geosynthetic Reinforced Alternative Subballast Material in a Railway Track. Geosynthetics International, v. 15, p. 311-321.

Gardoni, M.G., 2000. Hydraulic and filter characteristics of geosynthetics under pressure and clogging conditions. PhD. Thesis, University of Brasilia, Brasilia, 313 p. (in Portuguese).

Geo-Slope (2007), "Stability Modeling with Slope/W 2007 – An Engineering Methodology", Geo-Slope International Ltd, Calgary, Canada.

Geroto, R.E. (2008) Performance of Geomembrane Protecting Layers. Master Dissertation, Depto. de Geotecnia – EESC, University of São Paulo, 188 p. (in Portuguese).

Ghionna, V. & Jamilkowiski, M. (1981). Colonne di ghiaia. In: X Ciclo di conferenze dedicate ai problemi di meccanica dei terreni e ingegneria delle fondazioni metodi di miglioramento dei terreni. Politécnico di Torino Ingneria, atti dell'istituto di scienza delle construzioni, nº 507, 63p.

Gomes, R.C. (2007) Mining Tailings Disposal Systems Using Geotubes as Dewatering and/or Containment Structures, Proc. 5th Simp. Brasileiro de Geossintéticos /REGEO, Recife: ABMS/IGS-BR, CD (in Portuguese).

Gomes, R.C.; Martins, C.C. (2003). Design of Geotextile-Reinforced Structures with Residual Soils and Mining Residues in Highway Applications in Brazil. In: Proc. 12th Pan American Conference on Soil Mechanics and Geotechnical Engineering, 2003, Cambridge, Massachusetts. v. 2. , p. 1773-1778.

Gomes, R.C.; Saraiva, S.L.C (2010). Instrumental Analysis of Flexible Pavements Using Geosynthetics and Mining Residues. In: 9th International Conference on Geosynthetics, Guarujá, Brazil (submitted paper).

Junqueira, F. F.; Silva, A. R. L.; Palmeira, E. M. (2006). Performance of Drainage Systems Incorporating Geosynthetics and their Effects on Leachate Properties. Geotextiles and Geomembranes, England, v. 24, n. 5, p. 311-324.

Kempfert, H.G. & Gebresselassie, B. (2006), "Excavations and Foundations in Soft Soils", Springer-Verlag, Berlin, Germany, 576 pgs.

Kempfert, H.G., Stadel, M. & Kaeske, D. (1997), "Design of geosynthetic-reinforced bearing layers over piles", Bautechnik, 74 (12), 818-825

Koerner, R. M. (1998). "Designing with geosynthetics". Englewood Cliffs, New Jersey, Prentice Hall, 4th Ed.

Lodi, P.C. (2003) Some Topics about the Degradation of HDPE and PVC Geomembranes. Thesis. Depto. de Geotecnia – EESC, University of São Paulo, 284 p. (in Portuguese).

Lodi, P.C. , Bueno, B.S. & Vilar,O.M. (2008) UV exposure of polymeric geomembranes. Proc. of the 4th Asian Reg. Conference on Geosynthetics, June 17 - 20, Shanghai, China.

Lodi, P.C., Bueno, B.S. & Vilar,O.M. (2008) Evaluation Of Geomembrane UV Degradation Using Melt Flow Index And Oxidative Induction Time Tests. Proc. of the 4th Asian Reg. Conference on Geosynthetics, June 17 - 20, Shanghai, China

Low, B.K., Wong, H.S., Lim, C. & Broms, B.B. (1990), "Slip circle analysis of reinforced embankments on soft ground", Geotextiles and Geomembranes, 9 (2), 165-181

Maccaferri (2006) (http://www.maccaferri.com.br/ imagens/fotos/tupy.pdf, access 08/19/2009)

Magnani de Oliveira, H.M, Almeida, M.S.S. & Ehrlich, M. (2010), "Behaviour of two reinforced embankments on soft Clay", International Conference on Geosynthetics, Guaruja, Brazil.

Magnani de Oliveira, H.M. (2006), "Behaviour of reinforced fill on soft soils taken to failure" (In Portuguese: Comportamento de aterros reforçados sobre solos moles levados à ruptura), D.Sc Thesis, COPPE, Federal University of Rio de Janeiro.

Maia, I. S.; Vilar, O. M. The influence of some urban waste degradation agents on the mechanical properties of geomembranes. In: 7th International Conference on Geosynthetics, 2002, Nice: Balkema, 2002. v. II. p. 765-768.

Matheus, E. ; Palmeira, E. M. ; Agnelli, J. A. M.(2004). Degradation of some geosynthetics by UV radiation and temperature. Solos e Rochas - Revista Brasileira de Geotecnia, São Paulo, v. 27, n. 2, p. 177-188. (in Portuguese)

Mazon, A. (2009). Tailings Dewatering Techniques Using Textile Fences. Master´s Thesis, Graduate Program of Geotechnics, University of Ouro Preto, Ouro Preto, Brazil (in Portuguese).

Mesri, G. (1975), "Discussion: New Design Procedure for stability of soft clays, by Ladd and Foot, Journal Geot. Engineering Division, 101 (4). ASCE, USA.

Nahas, C. (2009) Personal information

Nascimento, M. T and Palmeira, E. M. (2002). Analysis of geomembrane damages in landfills. In: Proc. XII CBMSEG, São Paulo, ABMS, v. 2. p. 749-757. (in Portuguese)

Oliveira, F.J.P (2009) Personal information.

Palmeira, E. M. (2006) Geosynthetics in Drainage Systems of Waste Disposal Areas - Keynote Lecture. In: Proc. Int. Symp. on Technology and Treatment of Solid Waste, Rio de Janeiro. Rio de Janeiro: COPPE/UFRJ, v. 1. p. 1-15.

Palmeira, E. M.; Beirigo, E.A. ; Almeida, M.G.G. (2009). Tailings-Nonwoven Geotextile Filter Compatibility in Mining Applications. Geotextiles and Geomembranes, v. 27, p. 1-27.

Palmeira, E. M.; Remígio, A. F. N.; Ramos, M.L.G.; Bernardes, R. S. (2008) A Study on Biological Clogging of Nonwoven Geotextiles under Leachate Flow. Geotextiles and Geomembranes, v. 26, p. 205-219.

Palmeira, E.M., Gardoni, M.G., Luz, D.W.B. (2005). Soil-geotextile filter interaction under high stress levels in the

gradient ratio test. Geosynthetics International 12, (4), p. 162-175.

Raithel, M. (1999). "Zum trag und verformungsverhalten von geokunststoffummantelten sandsäulen", Schriftenreihe Geotechnik. Universität Gh Kassel, Heft 6. Kassel, Germany.

Raithel, M., Kirchner, A., Schade, C. & Leusink, E. (2005), "Foundation of Constructions on Very Soft Soils with Geotextile Encased Columns – State of the Art, GSP-136 Innovations in Grouting and Soil Improvement, "Geo-Frontiers", ASCE, Austin, USA

Raithel,M., Küster, V. & Lindmark, A. (2004), "Geotextile encased columns – a foundation system for earth structures, illustrated by a dyke project for a works extension in Hamburg", Nordic Geotechnical Meeting, Ystad, Sweden

Rebelo, K.M. W. (2008) Evaluation of Protection Layers of HDPE and PVC Geomembranes. Doctor Thesis. Depto. de Geotecnia – EESC, University of São Paulo, 247 p. (in Portuguese).

Rowe, R.K. & Li, A.L. (2002), "Geosynthetic-reinforced embankments over soft foundations", 7th International Conference on Geosynthetics, Nice, France.

Sandroni, S.S, Lacerda, W.A. & Brandt, J.R.T. (2004), "Method of volumes for field stability control of fills on soft clay (in Portuguese)", Solos e Rochas, Vol 27, No.1, São Paulo, Brazil

Sandroni, S.S. and Deotti, L. (2008), "Instrumented test embankment on piles and geogrid platform at the Panamerican Village, Rio de Janeiro", 1st Panamerican Geosynthetic Conference, Cancún, Mexico

Santos, Queiroz and Vidal (2008), "Design techniques for Geotextile-Encased Columns – A Review", 1st Panamerican Geosynthetic Conference, Cancún, Mexico

Saraiva, S.L.C (2006). Methodology and Experimental Analysis on the Geotechnical Behavior of Substructure Highway Pavements. Master´s Thesis, Graduate Program of Geotechnics, University of Ouro Preto, Ouro Preto, Brazil, 123 p. (in Portuguese).

Schnaid, F. (2008), "In Situ testing in geomechanics", 352 pgs, Taylor and Francis, London, UK

Silva, A. R. L.; PALMEIRA, E. M.; VIEIRA, G. R. Large Filtration Tests on Drainage Systems Using Leachate. In: 4th International Congress on Environmental Geotechnics, 2002, Rio de Janeiro. Proceedings. Lisse: Balkema, 2002. v. 1. p. 125-128

Silva, M.T.N; Palmeira, E. M.; Silva, F. A. R.; Sales, M.J.A. (2007). Analysis of chemical degradation of geomembranes in environmental protection works. Proc. 5o. Simp. Bras. de Geossintéticos-Geossintéticos 2007/REGEO, Recife : ABMS/IGS-BR, 2007. v. 1. p. 1-6.

Spotti, A.P. (2006), "Piled reinforced instrumented fill on soft soil" (In Portuguese: Aterro estaqueado reforçado instrumentado sobre solo mole), D.Sc Thesis, COPPE, Federal University of Rio de Janeiro.

Van Impe, W.E. (1989). Soil improvement techniques and their evolution. Balkema, Rotterdam, Holland, pp.63-66.

Van Impe, W.F. (1985). Belgian Geotechnical Volume (published for the 1985 Golden Jubilee of the ISSMFE).

Vidal, D., Silva, A.E. & Queiroz, P.I.B. (2002), " Design of geosynthetic reinforcement for embankments on soft soil considering the strength increase of foundation soil due to consolidation", 7th International Conference on Geosynthetics, Nice, France.

Vidal, I.G. (2003) CTR Caieiras – Landfill for Class II residues. Proc. II. CD Anais Geossintéticos 2003 - Regeo 2003, Porto Alegre, Paper BEI004.(in Portuguese). references

Villard, P. Kotake, N. & Otani, J. (2002), "Modelling of reinforced soil in finite element analysis", 7th International Conference on Geosynthetics, Nice, France.